5-2005

Multi-walled carbon nanotube electrodes for sodium borohydride fuel cell

Kedar D. Deshmukh

MULTI-WALLED CARBON NANOTUBE ELECTRODES FOR SODIUM BOROHYDRIDE FUEL CELL

A thesis presented to Rochester Institute of Technology

In partial fulfillment of the requirements for the degree of Master of Science in Materials Science and Engineering

Kedar D. Deshmukh

May 2005

COPYRIGHT RELEASE FORM

I, Kedar Deshmukh hereby grant permission to the Wallace Memorial Library of the Rochester Institute of Technology, to reproduce my thesis in whole or in part. Any reproduction will not be for commercial use or profit.

Date: 09/23/05

Signature: K. Deshmukh

Multi-walled Carbon Nanotube Electrodes for Sodium Borohydride Fuel Cell

Kedar D. Deshmukh

Approved:

Santhanam K.S.V.

Dr. K.S.V. Santhanam (Advisor)
Center for Materials Science and Engineering

Accepted:

Santhanam K.S.V.

Dr. K.S.V. Santhanam (Director)
Center for Materials Science and Engineering

ACKNOWLEDGEMENTS

I would first like to thank my advisor Dr. K.S.V. Santhanam for providing me the opportunity to pursue my masters at RIT and for his continuous guidance all the way long. His valuable suggestions, remarkable ideas and outstanding scientific expertise have helped me immensely to give shape to my exciting research in nanotechnology and fuel cells.

I am also thankful to my committee members, Dr. Gerald Tackas, Dr. Massoud Miri and Dr. Benjamin Varela, for their guidance and help. Dr. V. Gupta for help with XRD recordings and Hoeganes Corporation for SEM and EDAX recordings.

I would like to thank Dr. Terrence Morill for awarding me with a teaching assistantship. A special thanks to Ms. Brenda Mastrangelo, Mr. Tom Allston, Mr. Glenn Robinson and all the staff members of the stockroom for their constant help and support. I am also grateful to all the teachers with whom I interacted as a student and a teaching assistant. Big thanks to my friends Daliana, Akshay, Manjiri, Swapnil, Tejas and Kunal for making my stay away from my family enjoyable.

Finally, I would like to thank my family members back home and in US. My aspirations would have never been complete without their continuous love and support.

ABSTRACT

Borohydride fuel cell has been constructed for the first time using multi-walled carbon nanotubes (MCNT), functionalized MWCNT, platinized MWCNT or polycarbzole (Pcz) as electrodes. The output characteristics of borohydride fuel cell with platinized MWCNT electrodes have been shown to be superior to the conventional graphite based borohydride fuel cells. The catalytic activity of platinized carbon nanotubes has also been established in this study.

The MWCNTs have been functionalized by refluxing in 60-70% nitric acid for a period of 12 hours. The functionalized MWCNTs were characterized by FTIR and TGA. Platinization of MWCNTs was carried out electrochemically from chloroplatinic acid. Platinization of the tubes was demonstrated through SEM and XRD. Cyclic Voltammetry was used to characterize the platinum in MWCNT.

Fuel cells were constructed using MWCNT of different forms as the anode and commercially available oxygen electrode as the cathode. The current values at different loads were measured and plotted to construct the "load curves". From this data, the power density maps were generated. The power output of borohydride fuel cell has been shown to be higher than the graphite based fuel cell. The performance of borohydride fuel cells with Pcz electrode could not be decisive as the polymer deposited on platinum was used in the experiments. The polymer tends to peel off with time due to hydrogen bubbles generated in the medium. In the short time of the cell operation, it produced open circuit voltage of 1.369 V that is about 50% more than the commercially available borohydride fuel cell. However, it was noticed that it functions well as the cathode material in the borohydride fuel cells.

PUBLICATION AND PRESENTATION

K. Deshmukh, K.S.V. Santhanam, Polymeric Electrode for Sodium Bororhydride Fuel Cell, Int. Conference on Fuel Cell, Engineering and Technology, P.503, 2004, ASME

K. Deshmukh, K.S.V. Santhanam, Polymeric Electrode for Sodium Bororhydride Fuel Cell, Presented at the Second Int. Conference on Fuel Cell, Engineering and Technology, Rochester, NY, 2004

TABLE OF CONTENTS

LIST OF TABLES

LIST OF FIGURES

CHAPTER 1

1. Introduction

Electrical power (electricity) is produced by a wide variety of ways such as thermal, hydro, nuclear, wind and fuel cells. Among these methods, power generation by fuel cell is considered to be the most efficient (efficiency of about 80%) and pollution free. Consequently the entire world is turning towards examining the feasibility of adopting the fuel cell technology for electric power generation. [1].

Fuel cells produce electricity through electrochemical reactions. Typically fuel cells have an anode and cathode separated by an electrolyte. In operation, a fuel such as hydrogen is fed into the anode and an oxidizer such as oxygen (or air) is fed into the cathode. One type of fuel cell is depicted in Figure 1.

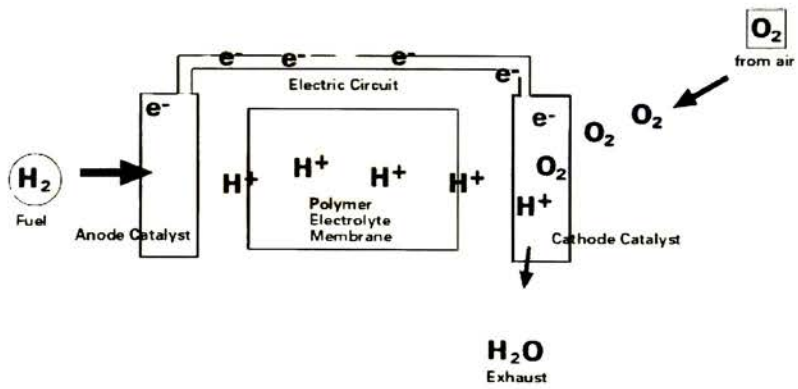

Fig.1: Hydrogen-oxygen fuel cell (www.fuelcell.org)

1.1 History of Fuel Cells:

In 1883, Sir, William Grove of Svensea, Wales invented the gaseous, voltaic battery, now referred to as fuel cell. He used two platinum electrodes, halfway, submerged in a beaker of aqueous sulfuric acid as an electrolyte, with tubes inverted over each electrode, one, containing hydrogen, the other oxygen.

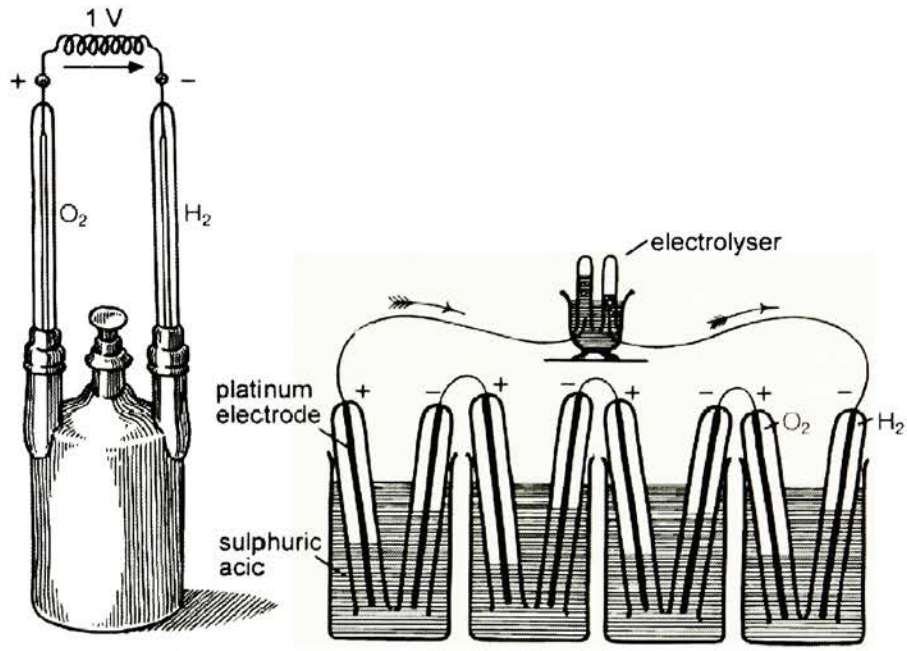

Figure 3. Grove's 'gas battery' (1839) produced a voltage of about 1 volt, shown left. Grove's 'gas chain' powering an electrolyzer (1842), shown right. (Photo courtesy of Berry, 2000)

Fig. 2. Grove's Gas Battery (www.fuelcells.org)

When the tubes were lowered, the gases displaced the electrolyte leaving only a thin layer of acid on the electrodes. A galvanometer connecting the two electrodes deflected indicating current flow. In 1889 Mond and Langer [1, 2] built the first prototype of the practical fuel cell (i.e. sustaining the fuel cell reaction) by solving the problem of electrolyte flooding (caused by the liquid electrolyte mixture in a matrix). They used a diaphragm to contain the sulfuric acid electrolyte. In 1937, Bauer and Preis [1, 2 and 3] developed the Solid Oxide Fuel Cell (SOFC). This was followed by the invention of the Alkaline Fuel Cells (AFC) in 1946 by Davtyan [1, 2 and 3] in Russia. Apollo space

mission had AFC fuel cells designed to operate at 27-31 V, 463-1420 W for at least 400 hours and provided water supply to the astronauts throughout the two-week mission to the moon in addition to electricity. Direct Methanol Fuel Cell (DMFC) was developed at Shell and Esso [1, 2 and 3] in 1965 to produce electricity with methanol as the fuel. In 1967, Pratt and Whitney [1, 2 and 3] developed the Phosphoric Acid Fuel Cell (PAFC) to use natural gas, but first reforming it to hydrogen. The Solid Polymer (proton exchange membrane) fuel cell was developed at General Electric in 1960 and provided on- board electric power due to the membrane degradation in the oxidative environment at the cathode electrode. This was corrected when DuPont invented Nafion membrane in 1972 [1, 2 and 3].

1.2 Characteristics and Advantages of Fuel Cell Systems

- High efficiency and reliability compared to batteries and other fuel sources. Efficiency can be very high (up to 70-80%) for the fuel cells with co-generation as compared to the system efficiency of current power generation, which is around 40-50%. [3,4]
- There are no moving parts in fuel cells and a very few parts in the fuel cell system so that it has higher reliability compared to an internal combustion engine or a gas turbine power plant.
- Fuel cell power plant emissions are at least 10 times lower than the most stringent California standards. They produce lower amounts of carbon dioxide and hence environmentally stable too.
- Since there is no combustion, fuel cells are quite too and do not produce noise pollution.
- Operating costs benefits include load following, power factor correction, quick response to generating unit outages, control of distribution line voltage and quality control.
- Control of power factor, line voltage and frequency can minimize transmission losses, reduce requirement for reserve capacity and auxiliary electric equipment.
- Fuel cell performance is independent of power plant size. The efficiency does not deteriorate going from MW to kW to W size power plants.

- Fuel cells do not require lengthy charging, just add the fuel and start immediately.
- A fuel cell running on methanol could power up to 20 times longer than traditional nickel-cadmium batteries in a comparable packaging size with a lower price and a small fraction of weight.

1.3 Different Types of Fuel Cells and their Electrochemical Reactions

Several different types of fuel cells are being examined for technological applications. The nature of the electrochemical reactions is different in each type and the following table gives the details. [1, 3, 4 and 5]

Table 1. Electrochemical Reactions in Fuel cells

Fuel Cell type	Anode Reaction	Cathode Reaction	Overall Reaction
Polymer Exchange Membrane Fuel Cell (PEMFC)	$H_2(g) \rightarrow 2H^+(aq) + 2e^-$	$\frac{1}{2}O_2(g) + 2H^+(aq) + 2e^- \rightarrow H_2O(l)$	$H_2(g) + \frac{1}{2}O_2(g) \rightarrow H_2O(l)$
Phosphoric acid Fuel Cell (PAFC)	$H_2(g) \rightarrow 2H^+(aq) + 2e^-$	$\frac{1}{2}O_2(g) + 2H^+(aq) + 2e^- \rightarrow H_2O(l)$	$H_2(g) + \frac{1}{2}O_2(g) + CO_2 \rightarrow H_2O(l) + CO_2$
Molten Carbonate Fuel Cell (MCFC)	$H_2(g) + (CO_3)2^- \rightarrow H_2O(g) + CO_2(g) + 2e^-$	$\frac{1}{2}O_2(g) + CO_2(g) + 2e^- \rightarrow (CO_3)^{2-}$	$H_2(g) + \frac{1}{2}O_2(g) + CO_2(g) \rightarrow H_2O(g) + CO_2(g)$
Solid Oxide Fuel Cell (SOFC)	$H_2(g) + O_2^- \rightarrow H_2O(g) + 2e^-$	$O_2(g) + H_2O(l) + 2e^- \rightarrow 2(OH)^-(aq)$	$H_2(g) + \frac{1}{2}O_2(g) \rightarrow H_2O(l)$
Direct Methanol Fuel Cell (DMFC)	$CH_3OH(aq) + H_2O(l) \rightarrow CO_2(g) + 6H^+(aq) + 6e^-$	$6H^+(aq) + 6e^- + 3/2\ O_2(g) \rightarrow 3\ H_2O(l)$	$CH_3OH(aq) + 3/2\ O_2(g) \rightarrow CO_2(g) + 2\ H_2O(l)$

1.4 Summary of Parameters

Table 2 gives the type of electrolyte used in the fuel cell, catalyst employed to drive the electrochemical reactions faster, operating temperature, membranes uses and application details. [1, 3, 4 and 5]

Table 2	*Operating*	*Details*	*Of Fuel*	*Cells*		
Fuel cells Parameters	PEMFC	DMFC	AFC	PAFC	MCFC	SOFC
Electrolyte	Polymer Membrane e.g. Nafion	Polymer membrane e.g. Nafion	Soln. of con. KOH in water (30-50%)	Liquid concentrated 100% Phosphoric acid	Hot and corrosive liquid molten carbonate (Li_2CO_3/Na_2CO_3) retained in a ceramic matrix of $LiAlO_2$)	Solid oxide ceramic Ytrium stabilized Zirconium dioxide (ZrO_2/Y_2O_3)
Operating temperature range (°C)	50- 100	25-90	50 – 200	150 -200	600-700	600-1000
Fuel on anode side	Hydrogen	Methanol	Hydrogen	Hydrogen	Hydrogen, Carbon monoxide, Methane	Hydrogen, Carbon monoxide
Catalyst	Pt, Pt/Ru	Pt on Cathode, Pt/Ru on anode	Platinum	Platinum	Nickel	Platinum, Pervoskite
Power density [kW/m^2]	3.8-6.5	0.4-0.6 at R.T, CO poisoning at higher temp	~1	0.8-1.9	1.5-2.6	0.1-1.5
Fuel efficiency %	50-60	20-30 Poisoning of catalyst.	50-60	50-55	55-65	60-65
Status of development	Demo. systems up to 50 kW	Demo. Up to 100 W, <10 W being developed for portable applications.	Up to 16 kW systems developed for space applications . Demo. Systems up to 300 kW	Most commercial systems operating at 200 kW, 11mW unit has been tested	Commercial and pre-commercial units are available in 250 kW, 1mW and 3mW	Demo. Systems up to 2MW.

1.5 Borohydride Fuel Cell Reactions:

In the above types of fuel cells (Table 2) the fuel used is hydrogen or methanol, methane. Several other fuels are being considered that would be advantageous in power generation. One such fuel is borohydride that can theoretically generate eight electrons. In comparison hydrogen oxidation can produce two electrons. Sodium borohydride is a water-soluble reducing agent, which oxidizes in aqueous alkaline media. The use of sodium borohydride as a fuel is interesting mainly due to the anodic reaction, which releases 8 electrons.

The reaction at anode is:

$BH_4^- + 8\ OH^- \longrightarrow BO_2^- + 6\ H_2O + 8\ e^-$ (1)

The corresponding reaction at cathode is:

$8\ e^- + 4\ H_2O + 2\ O_2 \longrightarrow 8\ OH^-$ (2)

The overall reaction is:

$BH_4^- + 2\ O_2 \longrightarrow BO_2^- + 2\ H_2O$ (3)

Reaction 3 is barely found to happen in practice because the anodic reactions on electrodes have to compete with the hydrolysis reaction as follows:

$BH_4^- + 2H_2O \rightarrow BO_2^- + 4H_2$ (4)

The actual anodic reaction will be as follows:

$BH_4^- + xOH^- \rightarrow BO_2^- + (x - 2)\ H_2O + (4 - 12\ x)\ H_2 + xe$ (5)

x here represents the actual number of the electrons released by each BH_4^- ion and it is called the columbic number

The fuel cell voltage is governed by the above reactions. For reaction (1) the standard potential is $E^o = -1.24$ V and for reaction (2), $E^o = 0.40$ V [6]. Hence the expected fuel cell voltage is 1.64 V. If the borohydride is hydrolyzed to produce hydrogen and hydrogen is oxidized as in the case of hydrogen-oxygen fuel cell, the expected voltage would be

reduced to 0.42 V, if operated as above without direct borohydride oxidation. On the other hand if operated as a fuel supplier to hydrogen-oxygen fuel cell, the expected voltage could be 1.23 V.

1.6 Advantages of Sodium Borohydride as a Fuel over other Fuel Cells [6, 7, 8]:

- A maximum of 8 electrons are available through electrochemical oxidation per borohydride molecule. Borohydrides also contain 10.6-wt % hydrogen, which is much more than hydrogen storage alloys. The hydrogen can be obtained by hydrolysis. Thus it can give higher energy density than other fuels.
- No gaseous products that would poison the catalyst.
- Sodium borohydride has low equivalent weight of 4.73 g.
- Sodium borohydride is chemically stable.
- Discharge products are water and sodium metaborate. Sodium metaborate can be converted back to coke by reducing it with coke and methane.
- The use of fuel soluble in electrolyte minimizes polarization at high current densities.
- It will not be necessary to rely on gas diffusion to transport reactants to the active sites. The circulating liquid can also serve as a heat transfer module.

1.7 Developments in Borohydride Fuel Cell:

Direct borohydride fuel cells were first proposed in early 1960 [7, 8]. Indig and Snyder [8] used sintered Ni anode (porosity 80%) and reported promising polarization behavior for BH_4^- oxidation in a 20 wt. % NaOH – 6 wt. % $NaBH_4$ electrolyte at 75 ^{O}C. At a current density 200mAcm^{-2} the anode potential was about -1.125 V versus Hg/HgO (i.e., -0.2 V vs. SHE) [8]. In another study, Jasinski [7] compared the electrocatalytic activities for KBH_4 oxidation of Pt, Pd and Ni_2B electrodes by investigating not only the polarization behavior but also the performance of borohydride fuel cells. The operating cell voltage of a KBH_4/O_2 fuel cell composed of a Ni_2B anode (effective surface area 25–30m^2 g^{-1}), Pt cathode and asbestos separator with a 2 wt.% KBH_4 25 wt.% KOH electrolyte, was 0.95 V at 45 .C for a current density of 100mAcm^{-2}. Under similar

conditions, but using a Pt anode (catalyst loading of 9mg cm^{-2}), the fuel cell voltage was somewhat lower, i.e., 0.87 V. In both studies [8], competing anodic hydrogen evolution was observed, lowering the columbic efficiency of BH_4^- oxidation to 40–49% on sintered Ni [8] and 70% in the case of Ni_2B, respectively [8]. The low current efficiency and accompanying H_2 evolution has been attributed to the four-electron oxidation of borohydride.

$$BH_4^- + 4OH^- \rightarrow BO_2^- + 2H_2 + 2H_2O + 4e- \quad (6)$$

In spite of the promising results reported in the 1960s, there has been a three-decade hiatus, as suggested by the lack of published information, in the research and development of borohydride fuel cells. Recently, Amendola et al., [6], developed a borohydride fuel cell using Au (97%)–Pt (3%) alloy electroplated on carbon cloth as anode while, the cathode was a commercial gas diffusion electrode separated from the anode by an anion exchange membrane [6]. The maximum power density reached was 63 $mWcm^{-2}$ at 70 °C, corresponding to a current density of 158 mA/cm^{-2}. Hydrogen evolution affected the columbic efficiency of the system and the number of utilized electrons was about seven out of a total of eight. In another recent approach, Li et al. proposed a Zr–Ni hydrogen-storage alloy ($Zr_{0.9}Ti_{0.1}Mn_{0.6}$ $V_{0.2}$ $Co_{0.1}$ $Ni_{1.1}$) as anode material, similar to those used in nickel–metal hydride batteries. Furthermore, these authors explored the possibility of using a cation exchange membrane as separator material in the alkaline borohydride fuel cell. The maximum power density was higher than in the work of Amendola et al., [6] e.g., 150$mWcm^{-2}$ at 300$mAcm^{-2}$ and 70 °C. However, hydrogen evolution was considered to be a major problem in spite of using a hydrogen-absorbing Zr–Ni alloy [9, 10]. The hiatus in the development of borohydride fuel cells might have been partly due to less intense research, as compared to studies involving other fuels relevant to power generation (e.g., H_2 and CH_3OH), directed toward understanding the complex electrode kinetic aspects of the BH_4^- oxidation as a function of electrode material and pH (for a review see Li et al. 2003). Regarding the pH effect, polarographic studies by Morris et al and Gardiner and Collatt [11, 12, 13] showed that for hydroxide per borohydride concentration ratios ($[OH^-]/[BH_4^-]$) greater than 4.4. The oxidation of BH_4^- on Hg electrode is an overall eight-electron process, characterized by a

half-wave potential $E_{1/2}$= 0.05 V vs. SHE. However, for concentration ratios [OH^-]/ [BH_4^-] less than 4.4, the hydrolysis of BH_4^- gains significance producing BH_3OH^-. The latter species is oxidized in a three-electron process, at potentials more negative than BH_4^-, as indicated by the $E_{1/2}$= -0.396 V vs. SHE.

$$BH_4^- + H_2O \rightarrow BH_3OH- + H_2 \quad (7)$$

$$BH_3OH^- + 3OH^- \rightarrow BO_2^- + 3/2\ H_2 + 2\ H_2O + 3e-. \quad (8)$$

The effect of electrode material is typically discussed in terms of 'catalytic' and 'non-catalytic' electrodes with respect to BH_4^- hydrolysis accompanied by H_2 evolution. In the case of Au, a 'non-catalytic' electrode, cyclic voltammetric studies by Mirkin and Bard [14] revealed a single voltammetric wave between -0.12 and +0.38V vs. SHE for BH_4^- oxidation in 0.2M and 1M NaOH electrolyte. Microelectrode investigations led to the conclusion that the BH_4^- oxidation on Au is an eight-electron process with the following reaction.

$$BH_4- + OH- \rightarrow BH_3^- + H_2O \quad (9)$$

$$BH_3 \leftrightarrow BH_3 + e- \quad (10)$$

It has been proposed that the monoborane (BH_3) formed is further engaged in fast reactions with OH^- and/or dimerization, yielding species, which are further oxidized to produce the total eight-electron wave [15]. Regarding the oxidation of BH_4 on 'catalytic' electrodes on the other hand, such as Pt, there is even less information. To our knowledge, there are only three previous studies of this process on Pt [15, 16, 17], the most recent one was published in 1989 [16, 17]. Elder and Hicking showed that Pt catalyzes the evolution of H_2 in contact with BH_4^- both at the open circuit potential and under anodic polarization conditions. Ivanov and Tsionskii [16,17] concluded, based on linear polarization experiments, that BH_4^- is electrochemically inactive on Pt in the potential region between -0.8 and -0.3V Vs. SHE, and the observed electrochemical response is due to the slow oxidation of surface-adsorbed hydrogen atoms formed by the

catalytic decomposition of BH_4^-. Recent work by Gyenge [18] showed that addition of an additive such as Thiourea (TU) at concentrations as low as 1.5mM effectively inhibits the catalytic hydrolysis associated with BH_4^- electro oxidation on Platinum. TU could improve the BH_4^- utilization efficiency and the columbic efficiency of direct borohydride fuel cells using catalytic anodes. Peak potentials between 0 and –2 V have been observed which indicate direct oxidation of BH_4^- and catalytic hydrolysis, which is otherwise evident between –0.7 and –0.9 V [18].

In another reaction the sodium borohydride solution hydrolyzes to yield H_2 gas and sodium metaborate ($NaBO_2$).

The reaction of $NaBH_4$ with H_2O is shown as follows:

$$NaBH_4 + 2H_2O \longrightarrow NaBO_2 + 4H_2 \qquad (11)$$

Koshima et al [19] have developed a 10 kW-scale hydrogen generator that generates high purity H_2 gas from aqueous solutions of $NaBH_4$. The generator was made up of a fuel tank for the $NaBH_4$ solution, a pump for the solution, the byproduct ($NaBO_2$) solution storage tank, a separator and a hydride reactor. The reactor contained a honeycomb monolith coated with Pt-$LiCoO_2$ catalyst. The maximum H_2 generation rate was 120 nl/min. The gravimetric and the volumetric H_2 densities of the system were 2 wt. % and 1.5 kg/l. In one of their papers, they have shown that the catalyst produced 100% of the theoretical amount of H_2 using excess water ($H_2O/NaBH_4$ = 210 mol/mol). Furthermore, it was demonstrated that $NaBO_2$ was recycled back to $NaBH_4$ using coke or methane [19]. In another study Amendola et al, 2000, used Ru catalyst for rapid hydrolysis of H_2 from sodium borohydride solution. The activation energy was 47 kJ/mole for the Ru catalyzed hydrolysis of $NaBH_4$. Hydrogen generated was equivalent of ~0.3 kW/g Ru catalyst at 25 °C and ~ 2 kW/g Ru catalyst at 55 °C [20].

1.8 Carbon Nanotubes (CNT)

1.8.1 Introduction

Carbon nanotubes (Fig.4) are fullerene like structures, which consist of long, thin graphene cylinders, closed at either end with caps containing pentagonal rings. These are large macromolecules that are unique for their size, shape, and remarkable physical properties. An ideal nanotube can be thought of as a hexagonal network of carbon atoms that has been rolled up to make a seamless cylinder. Just a nanometer across, the cylinder can be tens of microns long, and each end is "capped" with half of a fullerene molecule. They can behave like metals or semiconductors, can conduct electricity better than copper, can transmit heat better than diamond, and they rank among the strongest materials known. These intriguing structures have sparked much excitement in the recent years. A large amount of research in laboratories all over the world has been dedicated to the understanding of the physical and chemical properties of CNT [21-24].

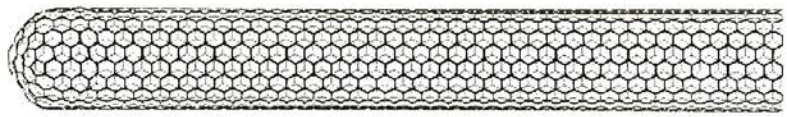

Fig. 3: Schematic of a CNT

(From http://www.personal.rdg.ac.uk/~scsharip/tubes.htm)

1.8.2 History

CNTs were discovered in 1991 by the Japanese electron microscopist Iijima [39, 40] of the NEC Laboratory in Tsukuba. He used high-resolution transmission electron microscopy to observe the material deposited on the cathode during the arc-evaporation synthesis of fullerenes. He found that the central core of the cathodic deposit contained a variety of closed graphitic structures including nanoparticles and nanotubes, of a type, which had never previously been observed. A short time later, Ebbesen and Ajayan, from Iijima's lab, showed how nanotubes could be produced in bulk quantities by varying the arc-evaporation conditions [41, 42]. Although Iijima's first observations were on multi-walled nanotubes, he also observed single-wall CNT two years later in 1993, succeeding the discovery by Donald Bethune and colleagues at IBM Almaden in California [42]. In

1996, for the first time, the Rice group, led by Smalley, synthesized bundles of aligned single-wall CNT. [37].

1.8.3 Types of CNT

Single Walled CNT (SWCNT)

A SWCNT can be thought of as a graphene sheet (Fig.4) rolled over to form a seamless cylinder [31]. The diameter of a SWCNT is 0.7-5 nm. A SWCNT can be as long as several hundred microns.

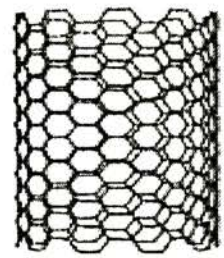

Fig. 4: Schematic of a SWCNT

Multi Walled CNT (MWCNT)

These nanotubes have thicker walls, consisting of several coaxial graphene cylinders separated by a spacing that is close to the interlayer distance in graphite (Fig.5) [31]. The outer diameters of MWCNTs are 2-25nm and the inner hollows are 1-8nm.

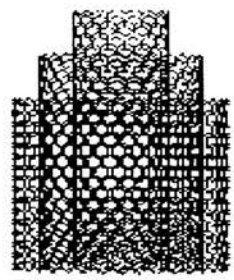

Fig.5: Schematic of a MWCNT

Structure of CNTs

There are many ways for a sheet of graphite to roll up into a perfect tube (Fig.6). The tube's electrical conductivity depends on the alignment of the carbon atoms. The different types are most easily explained in terms of the unit cell of a MWCNT- in other words, the smallest group of atoms that defines its structure. The chiral vector of the nanotube, C_h, is defined by $C_h = n\hat{a}_1 + m\hat{a}_2$, where $\hat{a}_1$ and $\hat{a}_2$ are unit vectors in the two-dimensional hexagonal lattice, and n and m are integers. Another important parameter is the chiral angle, which is the angle between C_h and $\hat{a}_1$.

Zigzag tubes have carbon bonds that zigzag down their length, which makes them good conductors of electricity, even better than regular metals. Zigzag nanotubes are formed when both n or m values are zero, and the chiral angle is 0°. Armchair tubes have carbon bonds that are perpendicular to the length of the tube. They behave like semiconductors, which either conduct or don't conduct electricity based on the surrounding environment. These nanotubes are formed when $n = m$ and the chiral angle is 30°. All other tubes, with chiral angles intermediate between 0° and 30°, are known as chiral nanotubes. [41, 44]

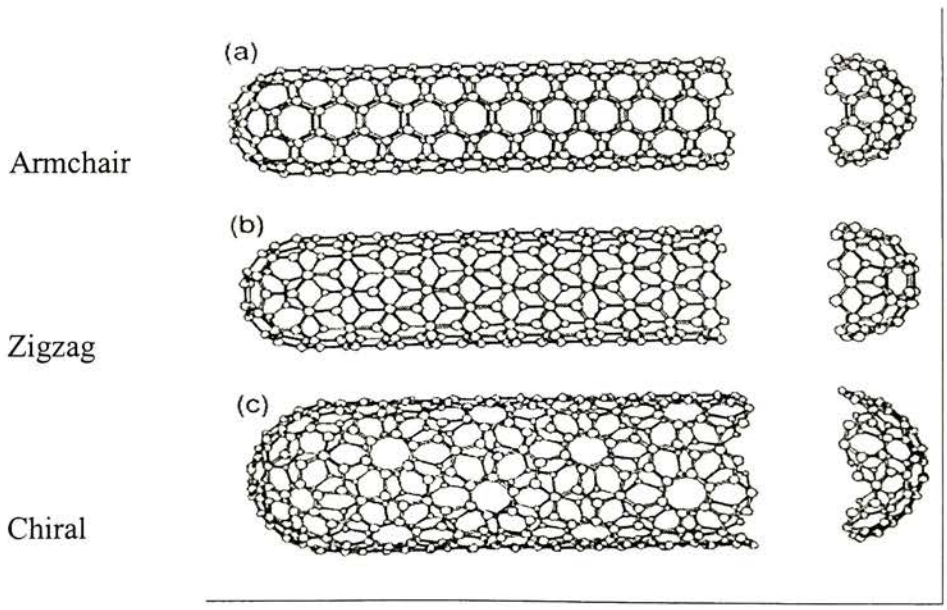

Fig. 6: Schematic of types of CNTs

1.8.4 Synthesis

The CNTs can be synthesized by the following methods:

1.8.4.1 Arc Discharge Techniques

This is one of the foremost methods for the synthesis of CNTs [31]. In this method, two graphite electrodes are placed about a millimeter apart. Typical electrode temperature is around 3000-4000 K. An arc is generated across the electrodes by a large DC current of 50-300 A (10-30 V) in a He atmosphere at pressures of 50-760 Torr. After discharging for an hour, a deposited carbon rod builds up at the end of the cathode. The cross-section of the rod consists of three regions- a gray core, a black ring and an outer gray shell. The black ring is the part with the CNT formed in a bundle called the 'buckybundle'. The gray regions are amorphous carbon. This method is an unclean process and also difficult to handle because of the soot which can be easily airborne. Efficient cooling is required for doping graphite electrodes with transition elements like Fe, Co, or Cu can produce homogeneous deposition of CNTs. [32, 42, 43, and 45].

1.8.4.2 Laser Ablation Method

In this method a scanning laser beam, 300 mJ/pulse at 532nm is focused to a 6-7 mm diameter onto a metal graphite composite target [32]. The laser beam scans across the target surface to maintain a smooth uniform face for vaporization. The target is supported by graphite poles in a 1-inch quartz tube evacuated to 10 mtorr and then filled with 500 torr Ar gas flowing at 50 sccm. The tube is maintained at 1200°C. The soot produced is swept by flowing Ar gas from the high temperature zone, and deposited onto a water-cooled copper collector positioned downstream, just outside the furnace. The growth of nanotubes in this method proceeds by the condensation of pure carbon vapor. The nanotubes produced have a single wall and very narrow distribution of diameters. This method produces SWNTs with good purity. [32, 42, 43, 45]

1.8.4.3 Decomposition of Hydrocarbons.

This method involves the catalytic decomposition of hydrocarbons over a supported catalyst. The hydrocarbons such as acetylene or methane are allowed to flow over a surface, which has catalytic metal nanoparticles such as Co, Cu or Fe deposited on it. After catalytic decomposition of the hydrocarbon, the carbon atoms nucleate and grow on the metal particles. The temperature needs to be maintained at 600-800°C for formation of MWNTs and to 900-1200°C for SWNTs. [32, 33, 42, 43, and 45]

1.9 Properties

The combination of size, structure, and topology endows CNTs with important and unique properties [43].

- CNTs have very high aspect ratios (length to diameter ratio), as high as 100 to 1000. [25]
- They have large surface area of around 1000 m^2/g. [23,27,28,29]
- CNT can be either metallic or semi conducting depending on their helicity and diameter.
- They have very high temperature stability (up to 800 °C in air).
- Chemical stability of CNTs is excellent. [26]
- CNTs are diamagnetic and show a pronounced anisotropy of susceptibility.
- They have non-linear optical properties, which depend strongly on the diameter and symmetry of the tubes. [30].
- The mechanical strength and rigidity of CNTs is exceptional compared to that of any known material. The Young's modulus of SWNT is ~1 TPa [34] while that of MWNT is ~1.28 TPa [35]. A maximum tensile strength of ~30 GPa [36] has been reported for CNTs.
- CNTs have excellent electrical properties. Resistivity value is ~ 10^{-4} Ω-cm [36].
- Thermal conductivity of CNTs is ~ 2000 W/m/K [38].

1.10 Potential Applications

- AFM, STM, CFM probe tips [23, 28].
- Electrodes for rechargeable batteries, Fuel Cells [27, 30].
- Charge storage devices [25,28,29,30]
- Chemical and biosensors [26].
- Actuators and artificial muscles [26].
- Hydrogen storage devices [27].
- Supercapacitors [28, 29, 30].
- Molecular electronics and nanomachines.
- Aerospace applications.
- Large-Area Field Emission Displays
- Conductive coatings (courtesy Eastman Kodak Company)

1.11 Aim and Scope of the Thesis

A fuel cell reaction can be typified as a process of conversion of reactants to products. This conversion involves changes in enthalpies and is shown in Figure 7.

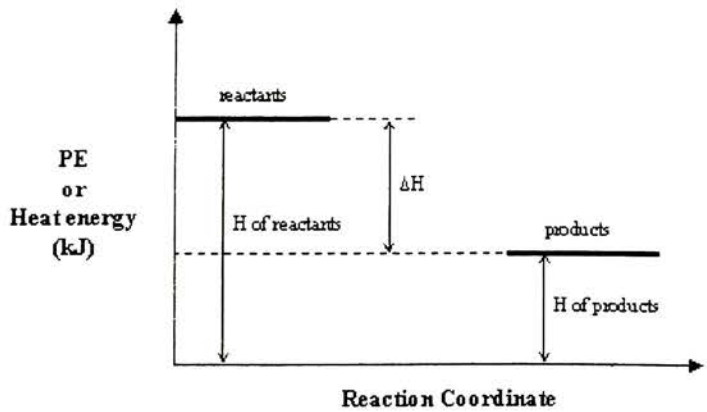

Fig.7: Energy diagram for a typical exothermic reaction

(http://www.chemcool.com/regents/kineticsequilibrium/aim4.htm)

At the anode sodium borohydride reacts, releasing energy. However, just because energy is released this does not mean that the reaction proceeds at an unlimited rate. The reaction has the classical energy form shown in figure 7. Although energy is released, the activation energy must be supplied to get over the activation barrier. If probability of a molecule having enough energy is low, then the reaction will only proceed slowly. Except at very high temperatures, this is indeed the case for fuel cell reactions [4].

There are three main ways to deal with the slow reaction rates:

- The use of catalysts
- Raising the temperature
- Increasing the electrode area.

The first two factors can be applied to any chemical reaction. However, the third is special to fuel cell and is very important. The rate at which the oxidation takes place on the fuel cell electrode is proportional to its area. Electrode area is such a vital issue that the performance of a fuel cell design is often quoted in terms of current per cm^2. However, the straightforward area (length * width) is not only the issue. Fuel cell electrodes are made highly porous so that it greatly increases the effective surface area. Modern fuel cell electrodes have a microstructure, which gives them surface areas that can be hundreds or even thousands of times, their straightforward area (length* breadth).

Multi-walled CNTs have larger surface area, as much as thousand times as compared to the conventional graphite [43, 44] that is used for making electrodes, they are highly electrically conductive and can reduce electrical loss in an electrode structure and provide greater cell design flexibility. The first report of using MWCNTs as an electrode material came in 1996 from a paper by Britto et al. (45). This work provided impetus to use of MWCNTs as electrodes. They also provide a means of increasing fuel cell current density at reduced catalyst loadings. Incorporation of highly conductive multi wall CNTs in one or both electrodes improves heat distribution and reduces temperature gradients. Porosity in the fuel cell electrode assemblies is a desirable attribute in order for fuel and oxidizing gases to reach the supported catalyst particles. CNTs can be made into structures that are permeable by liquids and gases. In sodium borohydride fuel cell, water is a diluent for the fuel, which means that water will be present on both the anode and the cathode. It is desirable for the fuel cell electrode material to have both high porosity and

hydrophobicity, so that water is not retained in the electrodes and impair the ability of the electrode to transmit gases. CNT surfaces are highly hydrophobic and can be fashioned into gas and liquid permeable forms such as mats and membranes. This would improve water transport in the fuel cell. Since temperature gradients in the fuel cell assemblies can reduce performance and lead to fuel cell failure, it is desirable for a fuel cell to be constructed in such a way that reduces such temperatures. Incorporation of highly, thermal conductive MWCNTs in one or both the electrodes, improves heat distribution and reduces temperature gradients [21].

This thesis is directed towards developing higher surface area electrodes for sodium borohydride fuel cells, using CNT. It reports the functionalization of the multi-walled CNT with concentrated nitric acid and metallization with catalytically active platinum. For comparison, electrodes made out of non-functionalized, functionalized and metallized CNT were made and tested for electrode properties. The functionalized electrodes provide a larger surface area and higher catalytic loading, resulting in higher current densities and power output for the fuel cell as compared to the commercially available catalytic graphite. Polymeric electrodes have also been studied as anodes or cathodes in fuel cells.

The electrodes were prepared in three combinations a) Non functionalized and non-metallized electrode b) Non-functionalized and metallized electrodes c) functionalized and metallized electrodes. They have been characterized using FTIR, TGA, X-Ray diffraction, Cyclic Voltammetry and SEM. The electrodes were fabricated in a micropipette using a binder. A prototype was constructed using metallized and functionalized CNTs.

The thesis is divided into four chapters. The first chapter is introduction to the review of developments. The second chapter gives the experimental details. This is followed by the experimental results and interpretations followed by the last chapter, which includes some work done on polymeric electrodes that would need further investigation.

CHAPTER 2

2 Experimental Details

2.1 Preparation of CNT electrode

A micropipette tip was used to hold the MWCNTs with the help of Nujol as the binder. 150mg of CNTs were used with 0.3gm of Nujol. The electrode was packed with CNTs to ensure good electrical contact. Copper wire was used as lead wire for electrical contact. The MWCNTs were obtained from Deal International Inc. and were 35% pure. They were synthesized by Laser Ablation method and were free from catalyst particles.

2.2 Functionalization of CNT

CNT are functionalized with concentrated nitric acid to improve the adhesion of the catalyst particles to the inner and outer walls of the MWCNTs. The functionalization with nitric acid (60-70%), results in hanging pendant –COOH groups, confirmed by FT-IR and TGA studies, which act as sites for binding of nano-Platinum particles. The MWCNTs were refluxed for 12 hours at 100 °C in 40ml of 60-70% nitric acid. The solid mass was removed my centrifugation for 60 min at 1500 rpm, after which they were washed with distilled water to remove the traces of acid and then were taken on a filter paper and dried in an oven at 80 °C for 3 hours.

2.3 Metallization of CNT

Metallization of MWCNT with platinum was done by the process of electro-deposition. The electro catalytic mass activity of Pt clusters in a periodic array of ordered nanoporous carbon is higher than that of platinum in carbon black samples, [58] and thus the former are suitable for borohydride oxidation. A 1.3mM solution of choloroplatinic acid in 0.5 M H_2SO_4 was used for electro deposition. The dried mass on MWCNTs was ultrasonicated in 50 ml of acetone for 30 min. The acetone was then decanted and allowed to evaporate. An electrode was fabricated using these nanotubes. The electro deposition was done in a standard three-chamber glass cell using Pt as counter electrode and SCE (Saturated Calomel Electrode) as the reference electrode. Gamray software version 3.11 was used to do the deposition using cyclic voltametry. The deposition time

was increased from 30 min to 300 min for increasing the amount of platinum deposition. The deposition curve for platinum is shown below. The platinum deposition is evident at the oxidation peak at 0.31V vs. SCE. (Fig.8)

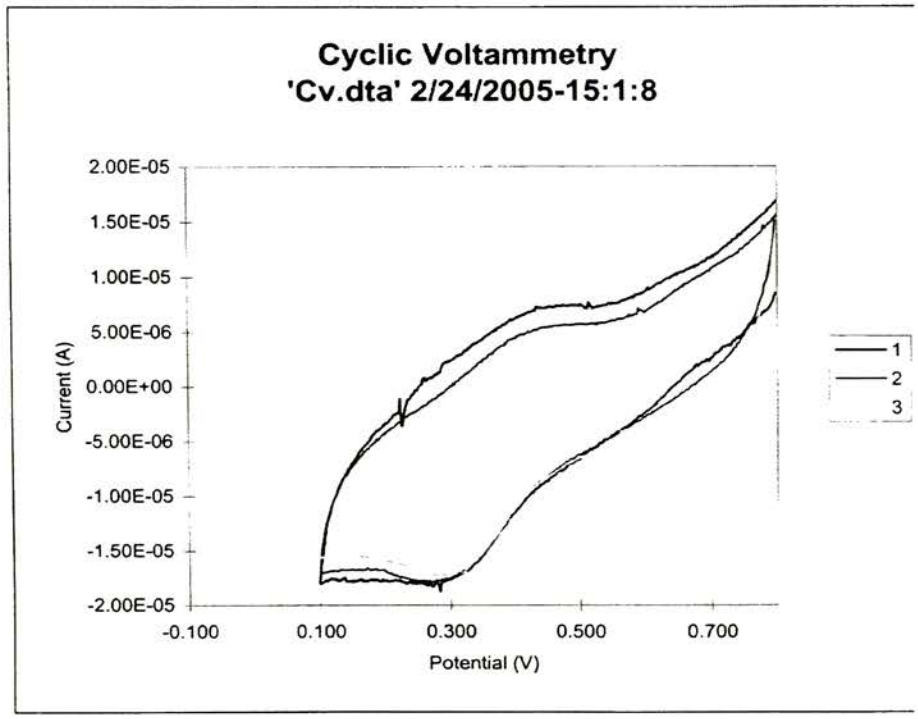

Fig.8: Platinum deposition on carbon nanotubes using the Gamray software.

2.4 Characterization Techniques

2.4.1 Fourier Transform Infrared Spectroscopy (FTIR)

IR spectroscopy is an invaluable tool in organic structure determination and verification. It is widely used for the characterization of functionalized CNT. The functionalization of the nanotubes was indicated by the presence of carboxylic acid peaks in the spectra of the functionalized MWCNTs. A Bio-Rad Excalibur Series FTS 3000 instrument was used to analyze the various samples using a diffuse reflectance cell. The spectra were obtained from 4000-400 cm^{-1} and 64 scans were obtained for each sample. The resolution was set at $4cm^{-1}$.

2.4.2 Cyclic Voltametry (CV)

CV is an electroanalytical method in which the current response of a small stationary electrode in an unstirred solution is excited by a triangular potential waveform. The current is measured as a function of potential. CV is used to study fundamental oxidation and reduction processes in various media, adsorption processes on surfaces, electron transfer mechanisms of chemically modified electrodes and for determining charge storage capacity of potential battery electrode materials. The electroanalytical cell consisted of three electrodes, immersed in solution containing an analyte. The working electrode was made of the MWCNT, a saturated calomel electrode was used as the reference electrode and graphite or platinum plate electrode was used as the counter electrode. A micropipette tip was filled with the MWCNT and used as the working electrode. The exposed area of the working electrode was around $0.2mm^2$. Gamray instruments framework version 3.11 software was used for CV.

2.4.3 Thermogravimetric Studies

The nanotubes before and after functionalized were analyzed by thermogravimetric analysis to determine whether the degradation temperature and characteristics change after functionalization. The thermogravimetric studies were done on TGA 2050, TA Instruments, using the ramp and isothermal hold method. The MWCNT sample was degraded under air at 1000 °C at a ramp rate of 10 °C /min. and was held isothermally for 20 min.

2.4.4 X-Ray Diffraction

X-Ray diffraction spectrum was recorded using Philips XRD spectrometer using CuKα1 radiation source. The 2θ reflections range was set from 15 to 90 degrees. XRD was used mainly to observe the evidence of Pt deposition on CNT and its behavior as a function of deposition time.

CHAPTER 3

3. Results and Discussions

The electrochemical oxidation of borohydride has been investigated previously. It is supposed to be a stepwise process [14], complicated by a stepwise hydrolysis reaction [15]. Therefore, there may exist several intermediates and different reaction routes for the oxidation of borohydride. For example, Elder and Hickling [16] proposed the following reaction scheme for the anodic behavior of borohydride on a smooth platinum surface.

Initial Step

$$BH_4^- + Pt - 2e \leftrightarrow Pt\cdots BH_3 + H^+ \quad (12)$$

$$Pt\cdots BH_3 + OH \rightarrow Pt\cdots BH_3OH^- \quad (13)$$

Rate-determining Step

$$Pt\cdots BH_3OH^- \; 2e \rightarrow Pt\cdots BH_2OH + H^+ \quad (14)$$

$$Pt\cdots BH_2OH + H_2O \rightarrow Pt + BH_2(OH)_2^- + H^+ \quad (15)$$

Slow Hydrolysis

$$Pt\cdots BH_3OH^- + H_2O \rightarrow Pt + BH_2(OH)_2^- + H_2 \quad (16)$$

Completion Step

$$BH_2(OH)_2^- + H_2O \rightarrow BH(OH)_3^- + H_2 \quad (17)$$

$$BH(OH)_3^- \rightarrow H_2BO_3^- + H_2 \quad (18)$$

3.1 Thermogravimetric analysis of MWCNTs

MWCNTs used here showed TGA characteristic as shown in Figure 9. At about 800°C a weight loss of 100% is reached indicating that no residue is left behind.

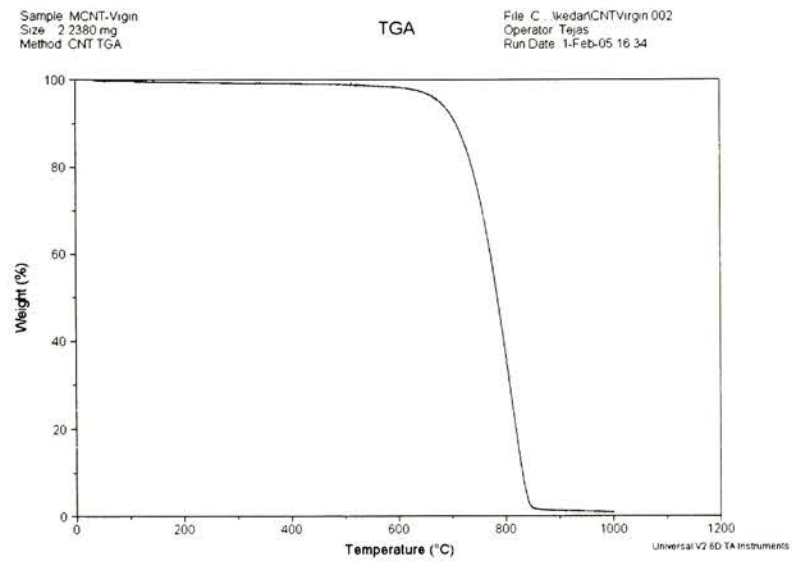

Fig.9: TGA of virgin MWCNT

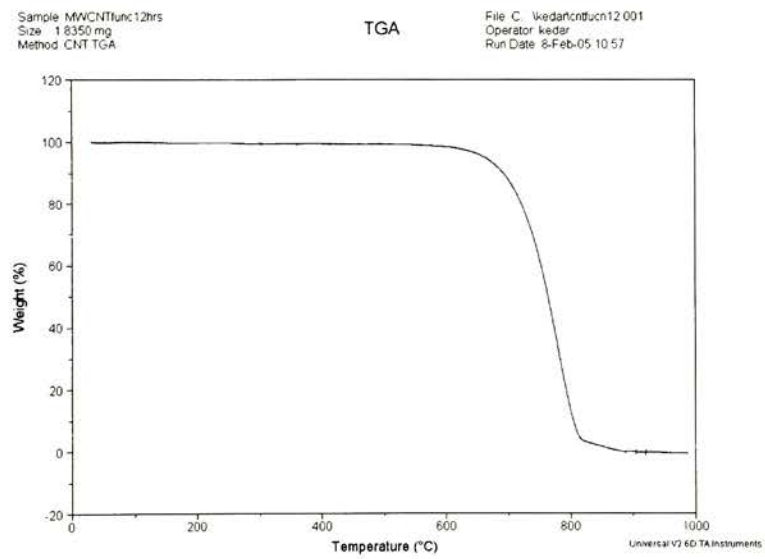

Fig.10: TGA of functionalized MWCNT

The nanotubes before and after were analyzed by thermogravimetric analysis to determine whether the degradation temperature and characteristics change during functionalization. Figure 10 shows the TGA graph of the core ground material as received and Figure 11 shows that of the functionalized CNT. The graphs show a change in slope in the two samples. The graph for functionalized MWCNT shows a higher slope

than that of the virgin CNT. This indicates a less amount of weight change with respect to temperature. The possible difference could be due to the carbonyl end groups that have been acquired during functionalization. It would be harder to oxidize the carboxyl groups than to oxidize pure carbon, causing the degradation time to increase with temperature.

3.2 Evidence for functionalization by FT-IR spectroscopy

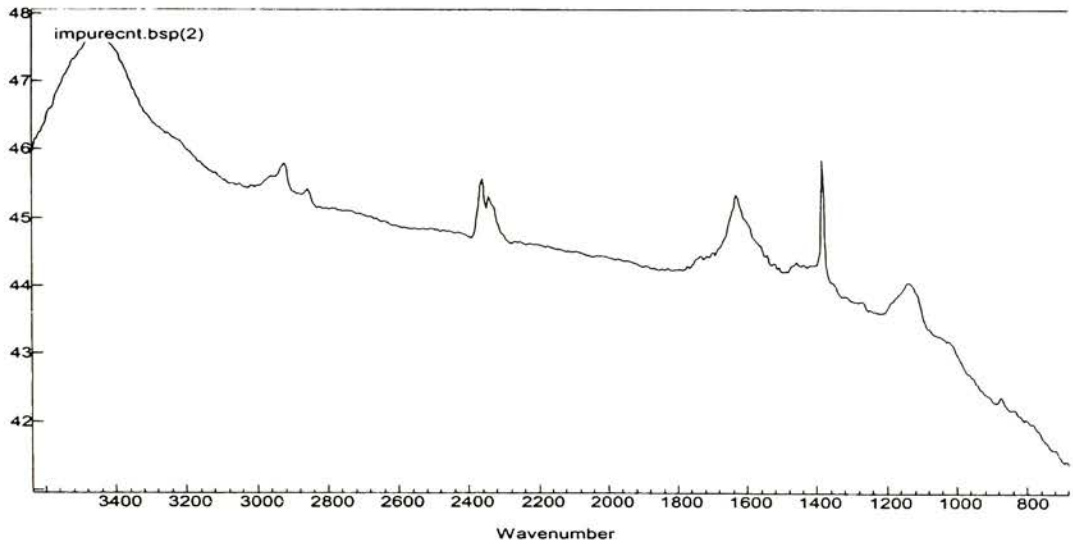

Fig.11: Non-functionalized MWCNT

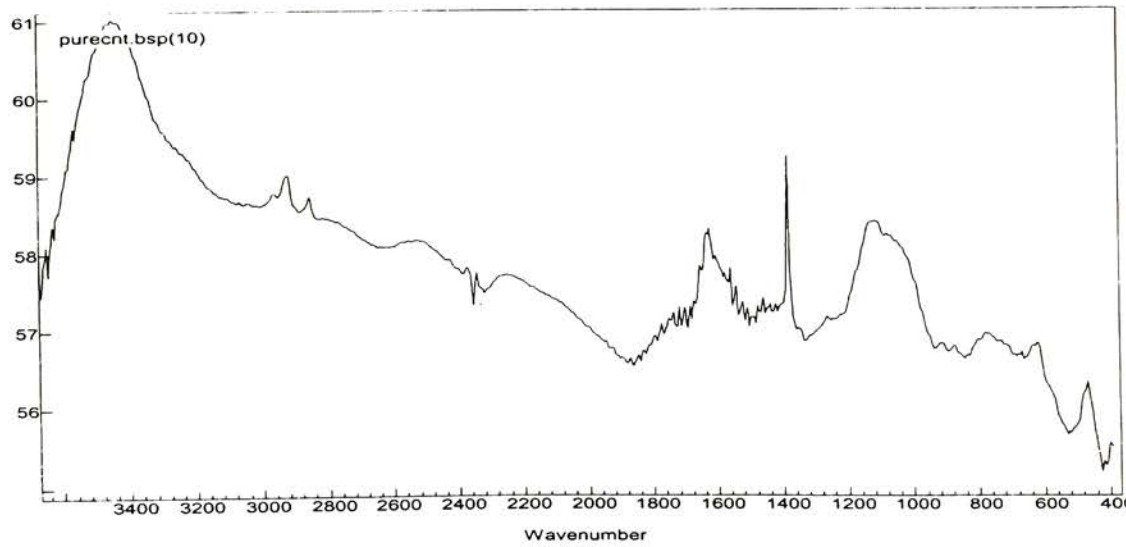

Fig.12: Functionalized MWCNT

Figure 11 shows the FTIR spectra of the virgin CNT. There is no peak in the range of 1700-1900 wave numbers, indicating no presence of carbonyl groups. Figure 12 shows the CNT after functionalization with nitric acid. There is a broad band in the range at 1700-1820 cm^{-1}, showing presence of carbonyl (C=O) group.

3.3 X-Ray Diffraction Analysis

CNT were examined by X-ray diffraction. The 2θ reflections are given in Figure 13. The observed pattern agreed with the one reported in literature [55]. Figure 13 shows the peak for MWCNT at 2θ = 25 deg as expected.

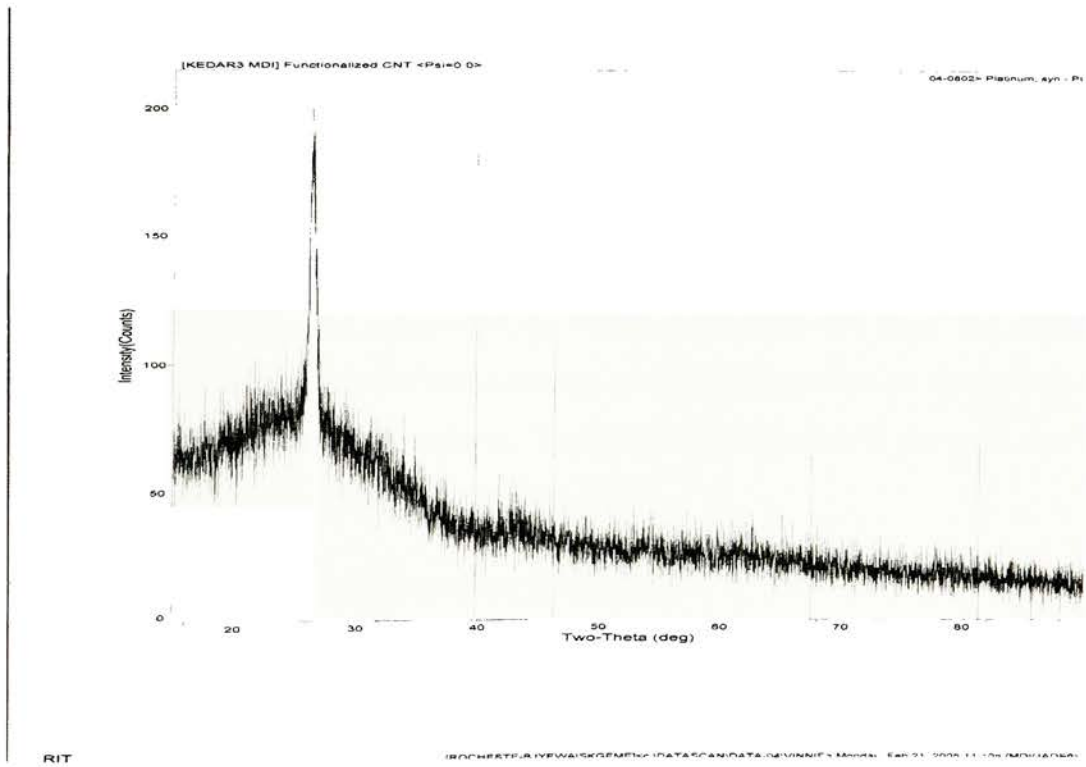

Fig.13: XRD pattern of FCNT without any deposited Platinum

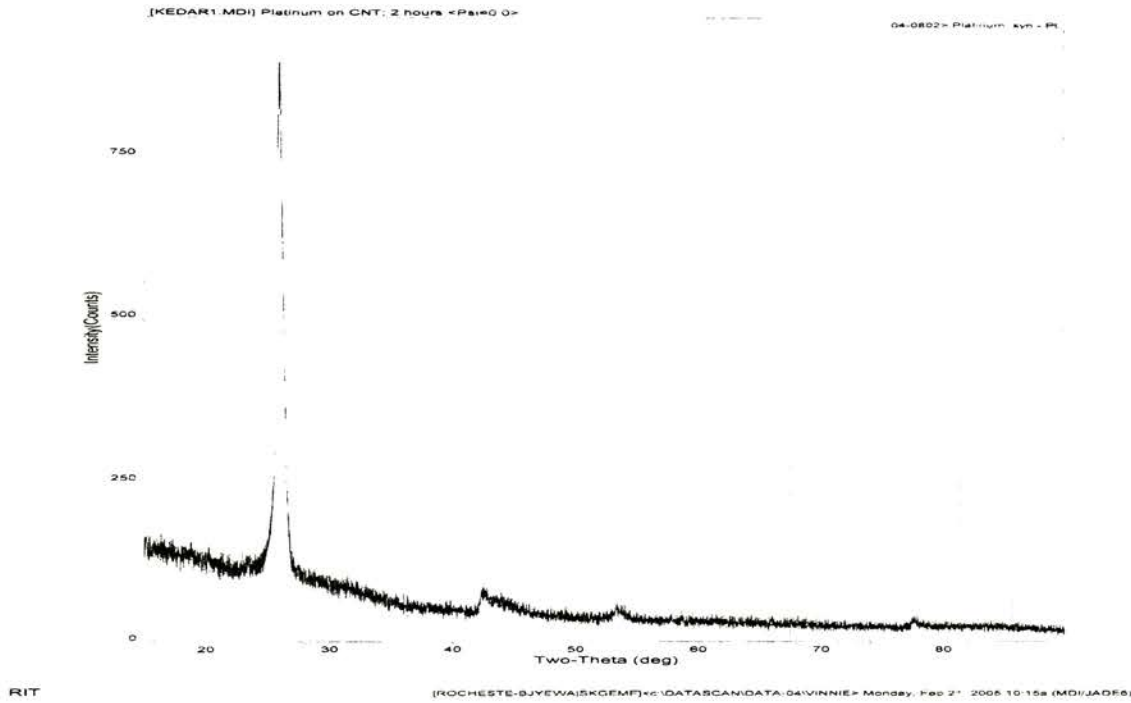

Fig.14: XRD image of FCNT with deposited Platinum

Figure 14, shows the XRD pattern for platinized CNT. The peak at 2θ = 44 deg is indicative of platinum and agrees with the literature data (2θ =40 deg). The shift in the peak is a result of the platinum being stressed or impurities present on the surface of the platinum due to the deposition process. The peaks at 2θ=54 and 78 are weak due to the small particle size of the deposited platinum. [55].

3.4 Scanning Electron Microscopy (SEM)

Figure 15 shows the SEM image of the platinized CNT. The platinization is evident by the highly reflective deposition on the outer walls of the dark contrasting particles of CNT.

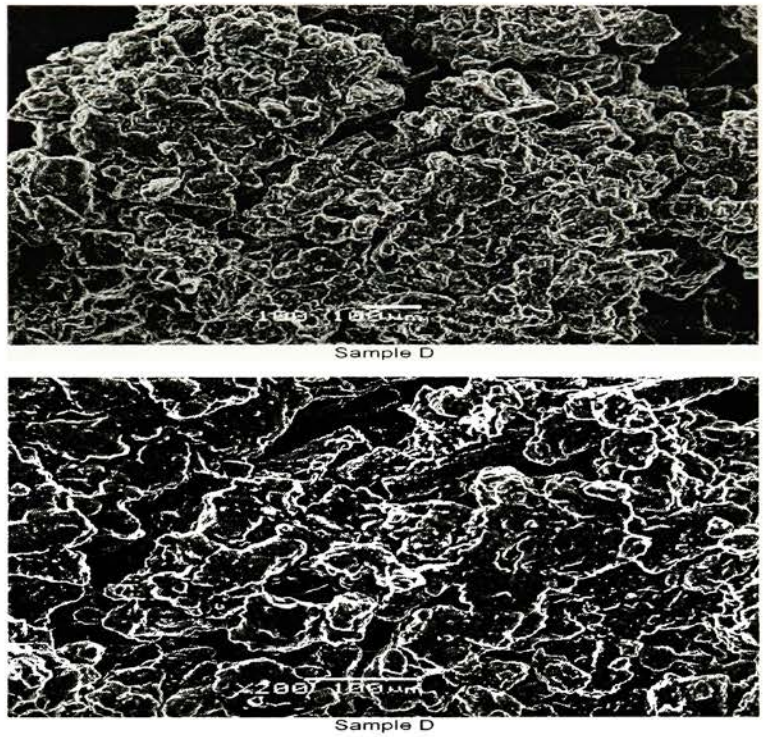

Fig.15: SEM image of platinized multi-walled CNT. Image above is at resolution of 100x and image below at 200x.

3.5 Surface Area Determination by Cyclic Voltammetry

The effective surface area of the electrode is determined by finding the peak current by cyclic voltammetry of the CNT electrode in ferrocynaide solution. The value of the peak current is put in the diffusion formula to get the effective surface area. [56, 57]

$$i_p = (2.65e5)*n^{3/2} * A* D^{1/2} * v^{1/2} * C \quad (19)$$

where,

i_p = peak current

n= number of electrons (=1 for ferrocynaide oxidation)

A= effective surface area of the electrode

D= diffusion coefficient (D= 0.76e-5 cm^2/s)

V= sweep rate

C= concentration

At a sweep rate of v= 20 mV/s, i_p= 6μA was obtained. Using this data and equation (19), the average surface area was calculated to be 0.036 cm^2.

3.6 Cyclic Voltammetric Oxidation of Borohydride at non-platinized MWCNT

The electrochemical oxidation of borohydride in 4M KOH medium, 10% wt/vol. of sodium borohydride was examined using non-platinized MWCNT electrode. The room temperature of the electrolytic solution was 22° C. These conditions were kept standard throughout the experimental work. The virgin MWCNT electrodes did not show any evidence for borohydride oxidation by CV. After functionalization of the MWCNT we could see not so well defined oxidation peaks in CV, although they are visible in the recordings at different sweep rates and different concentrations. Figures 16 and 17 show the cyclic voltammetric features of borohydride oxidation at sweep rates 10 mV/s and 100 mV/s respectively. The oxidation appears to be very slow. However, when the oxidation is carried out on platinum or platinized MWCNT electrode, the cyclic voltammetric features were improved and well-defined peaks were observed as shown by Figure 20.

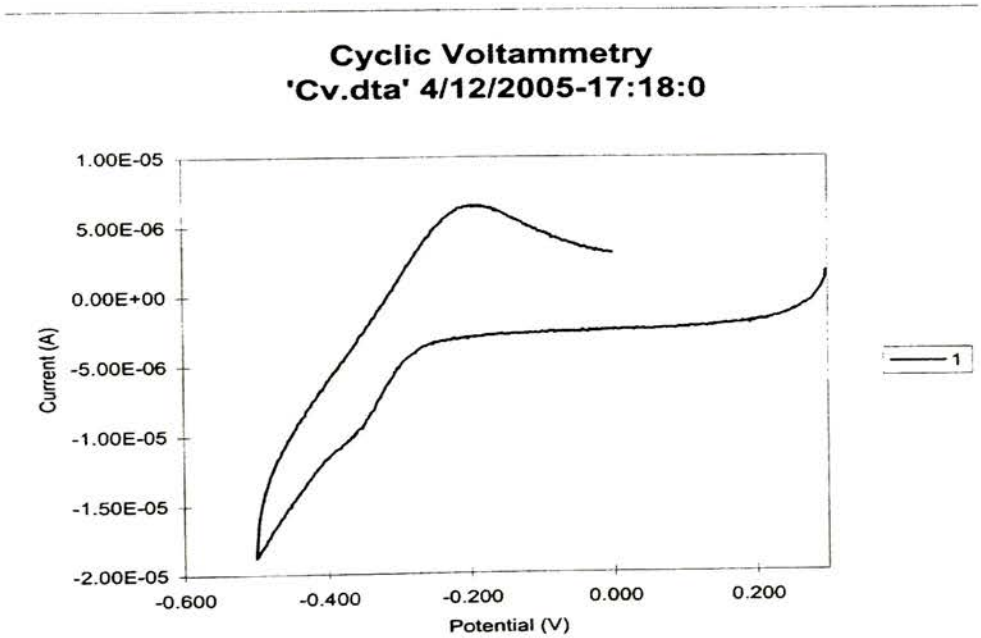

Fig.16: Oxidation of borohydride on functionalized, non-platinized MWCNTs. Concentration is 10 mg of sodium borohydride in 20 ml of 4M KOH.

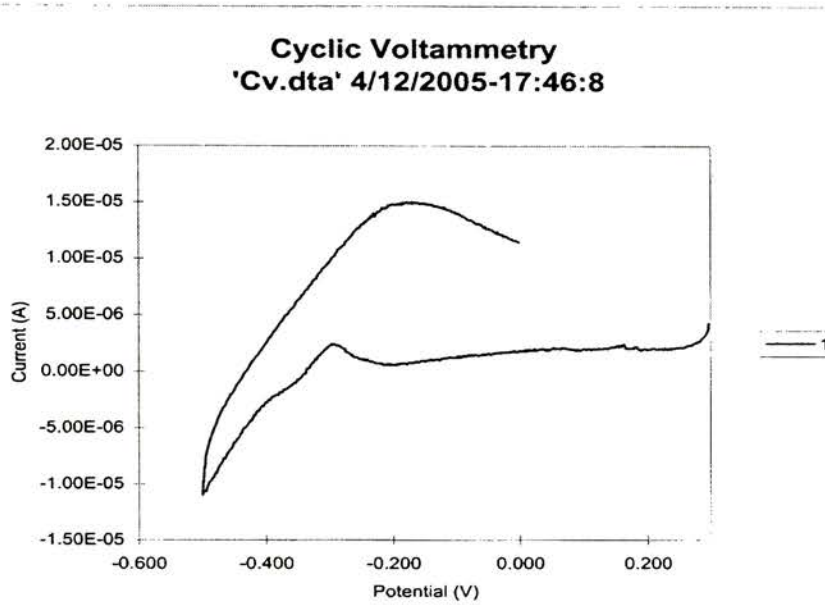

Fig.17: Oxidation of borohydride on functionalized, non-platinized. Concentration is 10 mg of sodium borohydride in 20 ml of 4M KOH. Sweep rate is 100 mV/s.

The cyclic voltammetric curves in Figures 16 and 17 show oxidation of sodium borohydride on functionalized, non-platinized CNT electrodes. The use of this material as anode in the borohydride battery resulted in the open circuit voltage for such a battery of 0.21V and the open circuit current of 9 μA. Load curves were obtained using variable resistor console. The cell was connected to variable resistor console, voltmeter and current meter. The output current was recorded with the varying voltage. The data is shown in table 3 below and the load curve depicted in fig.18.

Table 3. Current-Voltage data for load curve generation

Voltage (V)	Current (μA)	Current Density (μA/cm^2)
0.21	0	0
0.13	0.1	2.78
0.09	0.32	8.88
0.02	0.76	21.1
0	0.9	25

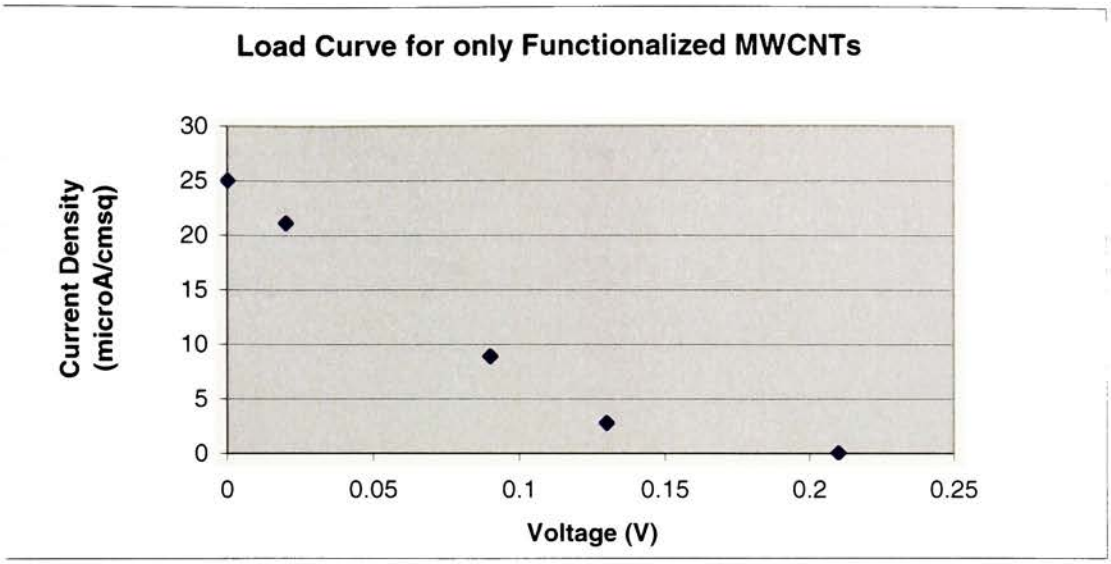

Fig.18. Load curve for functionalized MWCNT, borohydride fuel cell

3.7 Cyclic voltammetric Oxidation of Borohydride at Platinized MWCNT electrode

The oxidation of borohydride at CNT electrode is not distinctly visible in the cyclic voltammetric recordings carried out in the expected potential region of -0.6 to +0.30 V. However, platinized CNT electrode produced distinct anodic peak for borohydride (figure 20; compare it with figure 19 which is a background scan). In order to establish that the oxidation is due to borohydride, cyclic voltammetric curves were recorded for successively increasing concentration. In section 3.8, analysis of cyclic voltammetric curves is discussed. The current increase pattern suggests that the oxidation is diffusion controlled besides being due to the borohydride oxidation.

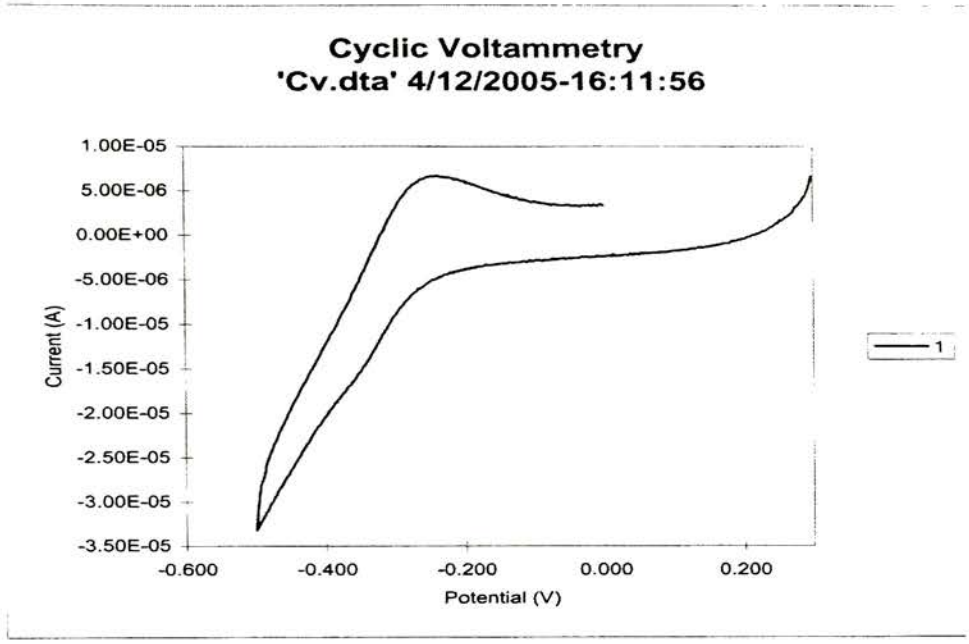

Fig.19: Background scan of platinized, functionalized CNTs in 4M KOH.

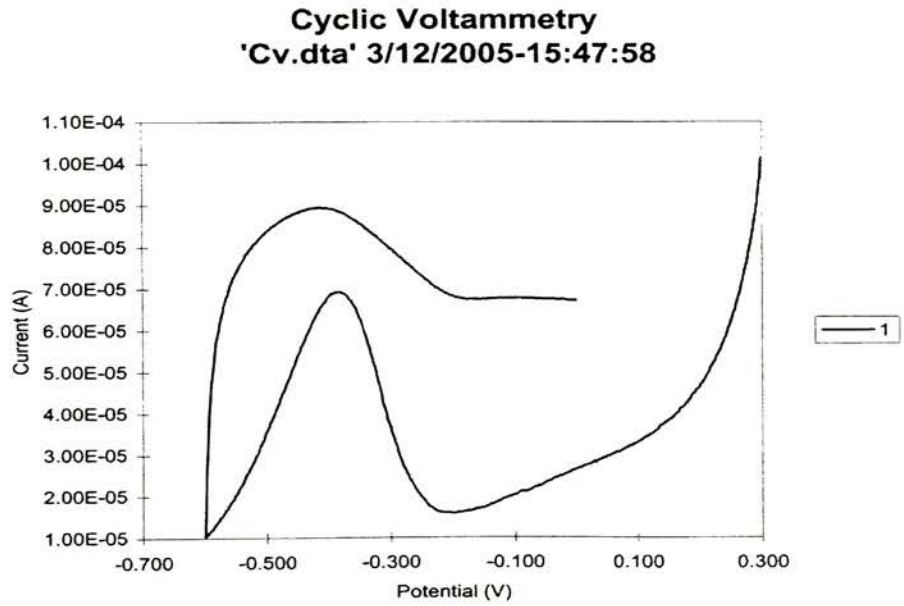

Fig.20: Oxidation of borohydride on platinized MWCNTs. Concentration is 10 mg of sodium borohydride in 20 ml of 4M KOH. Sweep rate is 10mV/s.

3.8 Analysis of Sodium Borohydride Oxidation Peak Observed in Cyclic Voltammetry using Platinized MWCNT

The cyclic voltammetric oxidation of borohydride in 4 M KOH produced the results shown in Table 4. Due to slow hydrogen evolution from the medium there is scatter in the data.

Table 4. Cyclic Voltammetric Oxidation of Borohydride in 4 M KOH medium at Platinized MWCNT

Conc NaBH4 mM	Sweep rate (mV/s)	E_{pc} (V)	I_{pc} (*10e-4A)	$I_{pc}/(\text{sweep rate})^{1/2}$ (10e-4)	$I_{pc}/$ (sweep rate)
6.60	10	-0.41	0.45	0.14	0.045
6.60	20	-0.44	0.30	0.067	0.015
6.60	50	-0.48	0.24	0.033	0.0048
6.60	100	-0.48	0.20	0.02	0.002
13.20	10	-0.39	0.60	0.18	0.06
13.20	20	-0.4	0.84	0.18	0.042
13.20	50	-0.43	0.55	0.077	0.011
13.20	100	-0.47	0.40	0.04	0.004
26.40	10	-0.43	0.90	0.28	0.09
26.40	20	-0.42	1.12	0.25	0.056
26.40	50	-0.41	1.18	0.16	0.0236
26.40	100	0.47	1.20	0.12	0.012
52.80	10	-0.38	2.41	0.76	0.241
52.80	20	-0.4	2.11	0.47	0.10
52.80	50	-0.42	1.47	0.20	0.03
52.80	100	-0.47	1.50	0.15	0.015

The current function data shows that the oxidation is more towards diffusion controlled than adsorption controlled. Figures 21 and 22 give the current function plot analysis. The data indicates that at slow sweep rates, the oxidation conforms more towards diffusion-controlled process; at higher sweep rates, the electrode response has not been fast. The different curves in the figures represent for different concentrations of borohydride in the medium.

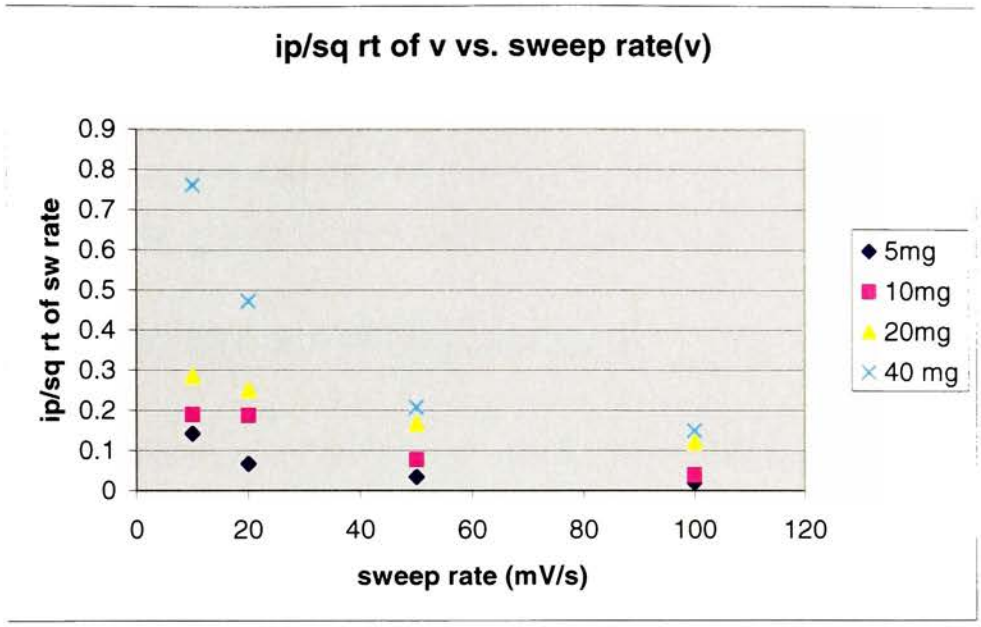

Fig.21: Plot of Current function with sweep rate 5 mg=6.60 mM; 10 mg= 13.20 mM; 20 mg=26.40 mM; 40 mg=52.8 mM.

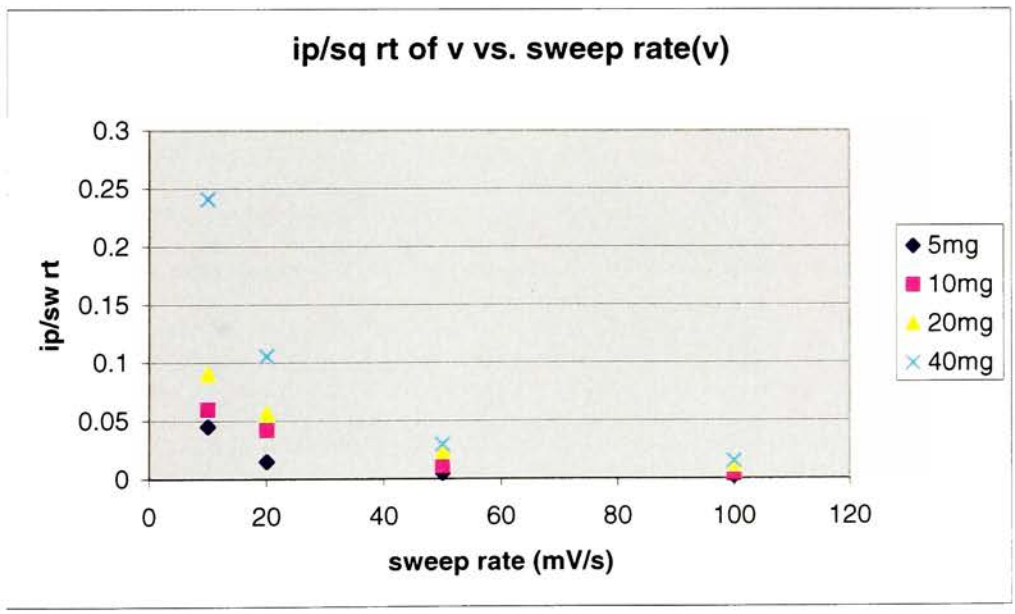

Fig.22: Plot of Peak Current normalized for sweep rate vs. sweep rate, 5 mg=6.60 mM; 10 mg= 13.20 mM; 20 mg=26.40 mM; 40 mg=52.8 mM.

3.9 Load Curve of Borohydride Fuel Cell with Non-Functionalized CNT

Borohydride fuel cell was constructed using CNT electrode as anode and commercially available oxygen (air) electrode as cathode in a tank containing 4 M sodium borohydride solution. The fuel cell configuration is shown below:

CNT (Pt)/ 4M $NaBH_4$/Membrane O_2/Pt (20)

The cell was connected to variable resistor console, voltmeter and current meter. Table 5, shows the current, voltage and power density data.

Table 5. Current density-Voltage Output of non-functionalized, metallized, borohydride-CNT Fuel Cell at room temperature

Voltage (V)	Current (mA)	Current Density (mA/cm^2)
		Area of the electrode = 0.036 cm^2
0.934	0.07	1.93
0.942	1.64	45.32
0.944	2.64	72.96
0.947	3.01	83.19
0.944	3.78	104.47
0.944	3.74	103.37
0.942	3.74	103.37

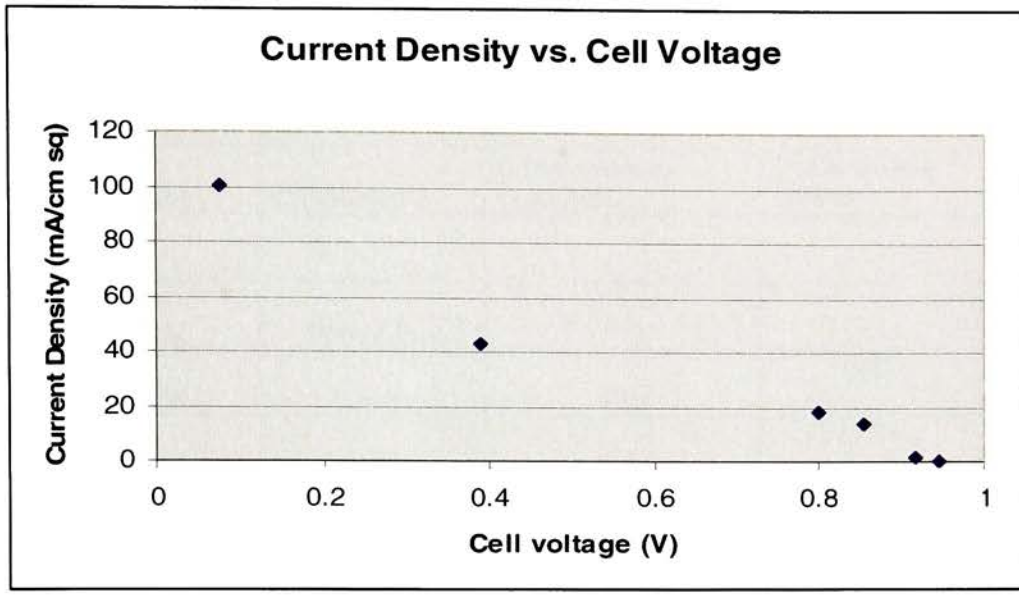

Fig.23: Load curve for platinized,non-functionalized CNT, borohydride fuel cell

3.10 Load curve of borohydride fuel cell with Functionalized CNT

In another modification of borohydride fuel cell, functionalized CNTs were used.

CNT(f)/Pt/ 4 M KOH/Membrane O_2/Pt (21)

The performance of this fuel cell was examined in the manner described in section 3.9. The current-voltage data is given in Table 6. The available current and voltages from this fuel cell are very similar to non-functionalized CNT. Consistently, the performance of this cell is better than the graphite based fuel cell.

Table 6. Borohydride Fuel Cell and Generation of Load Curve for Functionalized CNTs

Voltage (V)	Current (mA)	Current density (mA/cm2)	Power density mW/cm^2
0.952	Open circuit		
0.938	0.07	1.93	1.81
0.855	0.75	20.72	17.71
0.814	0.8	22.11	17.99
0.435	3.73	103.09	44.84
0.096	7.09	195.96	18.8

Figure 24 shows the load curve for the borohydride-CNT fuel cell. The maximum voltage that is obtained is 0.95 V. The voltage output is almost identical to the fuel cell operating with platinized graphite substrate. Amendola et al [6] reported the performance of borohydride fuel cells with highly dispersed gold/platinum particles supported on high surface area carbon silk (3.6 cm^2). They obtained a current density of 68 mA/cm^2 at 0.1 V and 50.0 mA/cm^2 at 0.40 V. Comparing this data with that in Table 2, the current output is nearly 2.8 times more than that has been reported in the literature. Besides Amendola et al obtained a maximum voltage of 0.90 V. Our group has thus obtained a voltage gain of 5.5% and current gain of 188% with borohydride-CNT fuel cell constructed here. The power output of this cell is also higher, around 44 mW/cm^2 compared with 20 mW/cm^2 reported in the literature [6]. Figure 25, shows a plot of power density as a function of voltage.

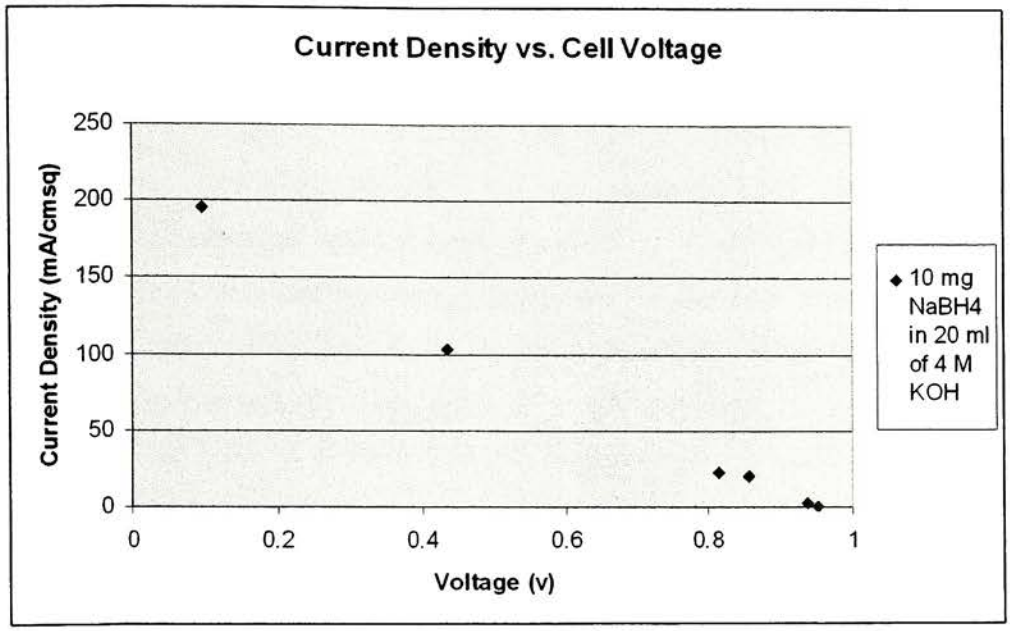

Fig.24: Load curve of borohydride Fuel cell constructed with functionalized CNT

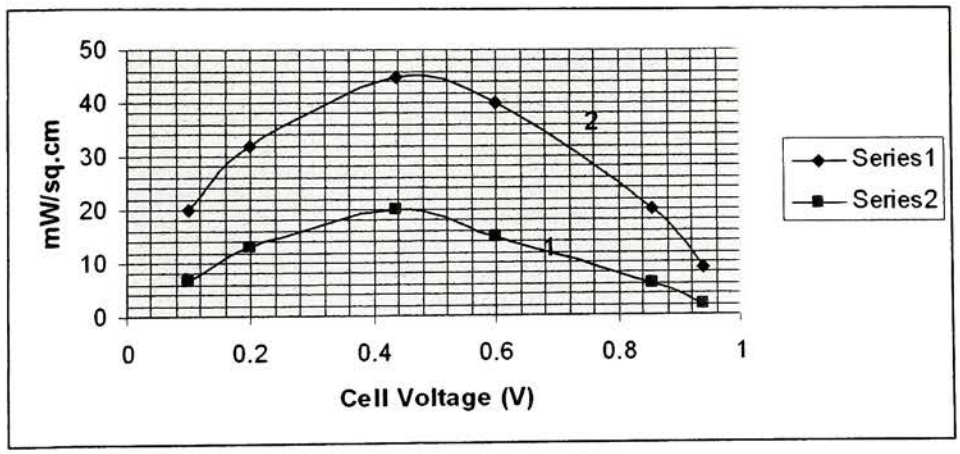

Fig.25: Power densities vs. voltage plot. Upper curve (solid line,) for borohydride-CNT fuel cell (present work). Lower curve: Taken from reference (4)

Figure 25, shows the load curve for this fuel cell. The power out put of the fuel cell is 44 mW/cm^2

3.11 Borohydride Oxidation at Polycarbazole (Pcz) Electrode

In an attempt to develop other fuel cell anodes that would overcome typical problems of cells, polycarbazole has been chosen [46-51] This polymer has the

3.11 Borohydride Oxidation at Polycarbazole (Pcz) Electrode

In an attempt to develop other fuel cell anodes that would overcome typical problems of cells, polycarbazole has been chosen [46-51]. This polymer has the highest oxidation potential and has been examined as an electrode material previously [50, 51, 52] for electrochemical work. The electrochemical oxidation of borohydride at Pcz electrode has been examined in 1M KOH electrolyte using cyclic voltammetry. Figure 26 shows the typical pattern obtained at this electrode. The cyclic voltammetric characteristics are given in Table 6. The data suggests that the oxidation of borohydride at the Pcz electrode is diffusion controlled. The oxidation of borohydride at the Pcz electrode increases with increasing sweep rate suggesting that it is ideal for the fuel cell. Fuel cells of the following types were constructed (note that in some cases, Pcz functions as cathode instead of as anode). The peak current is proportional to the concentration of borohydride in solution as depicted by the linearity of the data in Figure 27. The borohydride oxidation is thus proportional to its concentration.

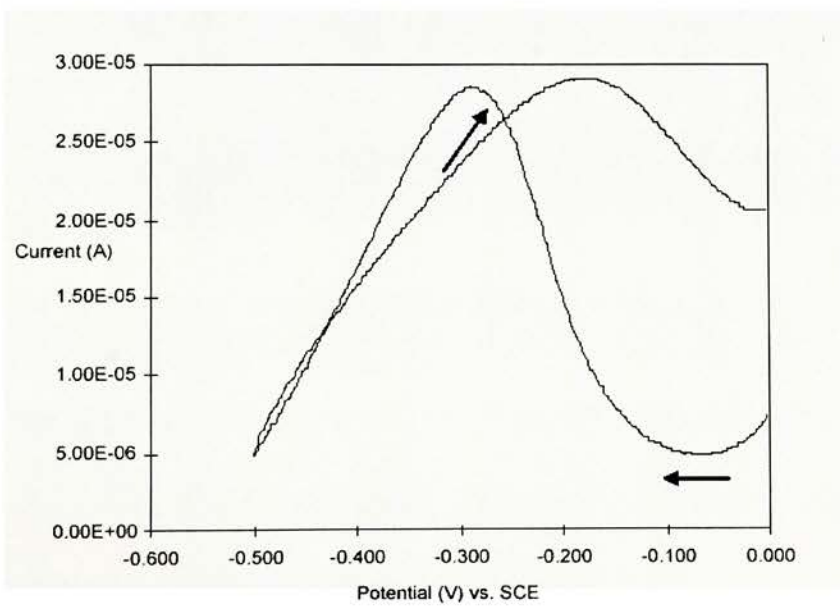

Fig.26: Cyclic voltammetric curve of sodium borohydride in 1M KOH at Pcz electrode. The potential is with respect to saturated calomel electrode. Sweep rate 10 mV/s. (Arrows indicate the direction of the voltage sweep).

Table 7. Cyclic voltammetric Oxidation of Sodium Borohydride in 1 M KOH at Pcz Electrode

Sweep rate (mV/s)	E_{pa} vs. SCE. (V)	I_{pa} (μA)
10	-0.292	28.50
20	-0.326	37.90
50	-0.314	45.00

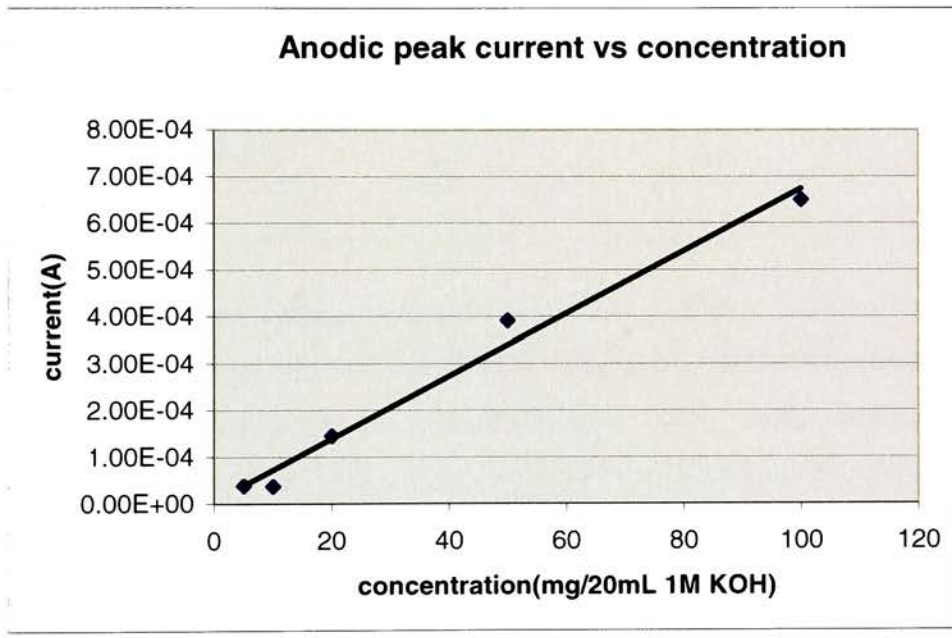

Fig.27: Plot of CV peak current vs. concentration of borohydride in solution.

3.12 Borohydride Fuel Cells with Polycarbazole electrode

Two types of fuel cells were examined here in the general configuration

Cathode | Fuel, Electrolyte | Anode

Pcz | $NaBH_4$, 1 M KOH, O_2 | Zn (22)

Cu | $NaBH_4$, 1 M KOH, O_2 | Pcz (23)

The open circuit potentials and potentials under different loads were studied and the results are given in Table 5..

Table 8. Fuel cell characteristics with Pcz electrode

Fuel Cell/Battery	**Voltage with $NaBH_4$ fuel, (V)**
Pcz and Zn electrodes with 1M KOH and $NaBH_4$, O_2	1.32
Pcz and Cu electrodes with 1M KOH, and $NaBH_4$, O_2	0.24

The open circuit voltage obtained in one cell is higher than the conventional electrodes used in borohydride fuel cell (0.90 V). The above cells were operated without any membrane separation between anode and cathode, which makes fabrication of the cell simpler for small current densities with reduced manufacturing cost. Cu electrode in borohydride fuel cell reduces the voltage-the mechanism is not clear and is being examined. The effect of concentration of $NaBH_4$ on the current-voltage behavior has also been studied. The results show promise for developing borohydride fuel cell using the new electrodes.

Borohydride fuel cells were constructed using Pcz electrode as cathode and platinum electrode as anode in 1 M K_2SO_4. The cell voltage reached a value of 1.369 V. With time, the voltage dropped and peeling off of the Pcz film occurred. This is attributed to the slow hydrogen evolution occurring in the medium. Hence load measurements could not be carried out. In another fuel cell configuration, Pcz electrode as anode and commercial oxygen electrode as cathode, the cell voltage reached about 0.484 V and the performance were similar to that described in section 3.9.

It has been demonstrated that borohydride is oxidizable directly at the Polycarbazole electrode. Other polymers like PEDOT/PSS, Polyaniline and Polythiophene have been examined previously for electrode materials and electrode supports for hydrogen-oxygen fuel cells [50, 53, and 54]. The anodic current is proportional to concentration of the borohydride in the medium. Fuel cells were constructed using the polycarbazole electrode using it as anode or cathode. Preliminary experiments carried out with borohydride cells demonstrate promising output voltages. Future work on constructing the load curves and power density maps would be useful in deciding the effectiveness of the polymeric borohydride fuel cells.

CHAPTER 4

4.0 Conclusions and Future Work

It has been demonstrated for the first time the utility of multi-walled CNT for Borohydride fuel cell. The performance of the platinized multi-walled CNT is superior to the existing technology. The current and voltage outputs are higher by 188% and 5.5%. [6]. Besides the power density from the MWCNT based fuel cell is more than two times the reported value in the literature [6]. Under some conditions the functionalized CNT performance is superior to non-functionalized carbon nanotubes. In the former case, insertion of carboxylic acid group is indicated by the Infrared spectroscopy. Platinization of the CNT is expected to anchor it on the surface providing an improved catalytic activity. This aspect needs to be probed further in the later studies by running the fuel cell for an extended period and measuring the performance characteristics.

Improved performance of the borohydride fuel cell with platinized CNT opens up interesting aspects on the nature of catalysis. Tubular geometry of the nanotubes with defect centers seems to provide better orientation of the metal for oxidative reactions. As the metal is deposited both inside and outside the nanotubes, the question arises as to which part produces better catalysis. All the results obtained here demonstrate that the overall catalysis is superior to the conventional platinized graphitic surface [6]. This opens up debate on an interesting aspect of planar geometry to curved geometry in fuel cell catalysis.

The current research has provided us with very interesting results. It would be exciting to examine other inexpensive catalytic materials in this type of fuel cells. Our research has shown the feasibility of CNT as a catalyst support material for fuel cells. It should be interesting to study borohydride fuel cells using SWNTs in place of multi-walled CNT Also further studies need to be done on developing theoretical models for borohydride oxidation on the catalyst bound to the surface of the CNT. Composites made form electrically conducting polymers and CNT could also prove useful as electrode materials.

REFERENCES

1. http://www.fuelcells.org

2. www.fuelcellstoday.com

3. R.K.Shah, S. G. Kandlikar, Fundamentals of fuel cell components and systems, June 16-18, 2003, ASME

4. J. Larminie, A. Dicks, Fuel Cell Systems Explained, John Wiley and Sons Ltd, 2003.

5. B.C.H. Steele, "Materials science and engineering: The enabling technology for the commercialization of fuel cell systems" Journal of Materials Science 36, 1053-1068, 2001

6. S.C. Amendola, P Onnerud, M.T. Kelly, P.J. Petillo, S.L., Sharp-Goldman, M.Binder, A novel high power density borohydride-air cell. J. Power Sources, 84, 130-133, 1999

7. M.E. Indig, R.N. Snyder, Sodium Borohydride, An Interesting Anodic Fuel. J. Electrochem. Soc., 109, 1104-1106, 1962.

8. R. Jasinski, Oxidation of Alkali Borohydrides- Eectrochem. Technol., 3, 40-43, 1965.

9. Z.P. Li, B.H. Liu, K. Arai, S. Suda, A fuel cell development for using Borohydride as the Fuel, J. Electrochem. Soc., 150, A868-872, 2003.

10. Z.P. Li, B.H. Liu, K. Arai, K. Asaba and S. Suda, Evaluation of alkaline borohydride solutions as the fuel for fuel cell, J. Power Sources, 126, 28-33, 2004.

11. J.H. Morris, H.J. Gysling, D. Reed, Electrochemistry of boron compounds. Chem. Rev., 85, 51-76. 1985

12. J.A. Gardiner, J.W Collat, Polarography of the tetrahydroborate ion: The effect of hydrolysis on the system, Inorg. Chem. 4, 1208-1212, 1965.

13. J.A. Gardiner, J.W. Collat, Kinetics of the stepwise hydrolysis of tetrahydroborate ion. J. Am. Chem. Soc., 87, 1692-1700. 1965.

14. M.V. Mirkin, A.J. Bard, Voltammetric method for the determination of borohydride concentration in alkaline aqueous solutions. Anal. Chem., 63,. 532-533, 1991

15. V. Mirkin, H. Yang, A.J. Bard, Borohydride oxidation at a gold electrode. J. Electrochem. Soc., 139, 2212-2217, 1992.

16. J.P.Elder, A.Hickling, Anodic Behavior of borohydride ion. Trans. Faraday Soc. Vol.58, 1852-1864, 1962.

17. M.V. Ivanov, M.V. Tsionskii, Anodic behavior of sodium tetrahydroborate on a platinum electrode. Electrokhimiya, 25, 514-516, 1989

18. M.V.Tsionski, M.V. Ivanov, V.M. Tsionski, Anodic oxidation of hydrogen on platinum at high pressures. Electrokhimiya, 25, 847-850, 1989

19. E. Gyenge, Electrooxidation of borohydride on platinum and gold electrodes: implications for a direct fuel cell. Electrochem. Acta, 49, 965-978, 2004

20. Y. Koshima, K Suzuki, K Fukumoto, Y Kawai, M Kimbara, H Nakinishi, S Matsumoto, Development of a 10 kW- scale hydrogen generator using chemical hydride. J. Power Sources,125, 22-26, 2004

21. S.C. Amendola, S. Sharp-Goldman, M. Januja, M. Kelly, P. Petillo, M Binder, An ultra safe hydrogen generator: aqueous, alkaline borohydride solutions and Ru catalyst. J.Power Sources, 85, 186-189, 2000

21. P.J. Britto, K.S.V. Santhanam, P. Ajayan, A. Rubio, Improved charge transfer on MWCNTelectrodes .Adv Mater, 11(2), 154-157, 1999

22. B.H.Liu, Z.P.Li, Seijirau Suda, Electrochemica Acta, 49, 3097-3105, 2004

23. S.S. Wong, J.D. Harper, P.T. Lansbury, C.M. Lieber, "MWCNT Tips: High-Resolution Probes for Imaging Biological Systems", *J. Am. Chem. Soc.* 120, 603-604, 1998

24. P. Ajayan O.Z. Zhou, "Applications of carbon nanotubes" in Topics in Applied Physics, 80, 391, 2001

25. J.Kong, M.R. Franklin, C.Zhou, M.G.Chapline, S.Peng, K.Cho, H.Dai, "Nanotube Molecular Wires as Chemical Sensors", *Science*, 287, 622., 2000

26. R.Baughman, C.Cui, A.A Zakhidov, Z.Iqbal, J.N Barisci, G.G Wallace, S.Roth,O.Jaschinki, "Carbon Nanotubes Actuators", *Science,* 284, 1340, 1999

27. R. Chahine, P. Bénard, "Metal Hydrides and Carbon for Hydrogen Storage", *IEA Task 12*, 2001.

28. E.K. Niu, R. Sichel, D Hoch, D. Moy, H. Tennet. High power electrochemical capacitors based on MWCNT electrodes, *Appl. Phys. Lett.* 70, 1480, 1997.

29. E. Frackowiak, K. Méténier, V. Bertagna, F Béguin, Supercapacitor electrodes from Multi-walled carbon nanotubes, *Appl. Phys. Lett.* 77, 2421, 2000.

30. E. Frackowiak, F. Béguin, Carbon materials for the electrochemical storage of energy in capacitors, *Carbon*, 39, 937, 2001.

31. D. Tomanek, R.Enbody, *"Science and applications of nanotubes"*, Kluwer Academic Publishers, New York, 1999.

32. T.Guo, P.Nikolaev, A.Thess, D.Colbert, R.Smalley, "Catalytic growth of single walled nanotubes by laser vaporization", *Chemical Physics Letters*, 243, 49, 1995

33. A.Fonsec, K. Harnandi, K.P Piedigrosso, J.F Colomer, P.A Thiry, J.B Nagy, "Synthesis of single and multi walled carbon nanotubes over supported catalysts", *Applied Physics*, 67, 11, 1998.

34. E. Dujardin et.al, "Young's Modulus of Single-Walled Nanotubes", *Physical Review B* 58(20), 14013-14019, 1998.

35. E. Hernández, Angel Rubio, *Nanotubes:* Mechanical and Spectroscopic Properties, (1999).

36. M.F Yu, B. S. Files, S. Arepalli, R.S. Ruoff, *Phys. Rev. Lett.* 84, 5552, 2000.

37. R.Smalley et.al, "Crystalline Ropes of Metallic Carbon Nanotubes", *Science*, 273, 483, 1996

38. J. Che, T. Cagin, W.Goddard III," Thermal Conductivity of Carbon Nanotubes".http://www.foresight.org/Conferences/MNT7/Papers/Che/; 13th Advancing Beneficial Nanotech, Oct. 22, 2005

39. S.Ijima, Helical Microtubes of Graphitic Carbon, Nature, 354, 56, 1991

40. S.Ijima, T.Ichibashi, "Single-cell carbon nanotubes of 1nm diameter", *Nature,* 363, 63, 1993

41. H.N. Singh (Ed.), *Nanostructured materials and nanotechnology,* Academic Press, 2001.

42. T.W Ebbesen, P.M Ajayan, "Large Scale Synthesis of Carbon Nanotubes," Nature, 358, 220, 1992

43. A. Thess, et al." Crystalline Ropes of Metallic Carbon Nanotubes." *Science*, 273, 483-487, 1996.

44. http://www.physicstoday.org/vol-56/iss-2/pdf/vol52no5p22-28.pdf

45. E.H. Hong, K.H. Lee, C.M. Ryu, J.H. Hun, J.E. Yoo, Method and apparatus for synthesisizing carbon nanotubes, Eur. Pat. Appl., EP 1190987, 2002

46. P. Chandrashekhar, Conducting Polymers, Applications and Fundamentals and Applications, Kluwer Academic Publishers, 1996

47. H.S. Nalwa (Ed.), Handbook of Conductive Moleculres and Polymers, Vol. 3, John Wilely & Sons, Ltd., Chichester, England, 1997.

48. T. Stokheim (Ed.), Handbook of Conducting Polymers, Dekker, 1986.

49. K.S.V Santhanam, N.Gupta, Conducting Polymer Batteries: Present and Future, Trends in Polymer Science, 1, 284, 1993.

50. P. Novak, K. Miller, K.S.V. Santhanam, O. Hass, Chemical Reviews, 97, 207-281, 1997.

51. R.N O'Brien, KSV, Santhanam, Electrochemica Acta, 32. 1209-1211,1987.

52. K. Nishio, M. Fujimoto, N. Yoshinaga, Nobuhiro Furukawa, O. Ando, H. Ono, T. Suzuki, Journal of Power Sources, 34,153-160, 1991.

53. Z. Qi, M. C. Lefebrve, P G. Pickup, Journal of Electroanaytical chemistry 459, 9-14, 1998.

54. A. Malinauskas, Synthetic Metals, 107, 75-83, 1999.

55. M. Adela, J. Angel, Nuclear Instruments & Methods in Physics Research, Section B, 97 (1-4), 11-15, 1997.

56. J.A Dean (Ed.), Lange's Handbook of Chemistry, 15th ed. McGraw- Hill, New York. 1999

57. A. J. Bard, L. R. Faulkner, Electrochemical Methods: Fundamentals and Applications, John Wiley and Sons Inc., 1980.

58. K.O Mc.Elrath, et al. Fuel Cell electrode comprising carbon nanotubes. US Patent Application 20040197638, Oct 7, 2004.